Pacific Northwest
NATIONAL LABORATORY

PNNL-30467

Hydrologic Evaluation of the Ringold Upper Mud Aquifer in the 100-H Area of the Hanford Site

September 2020

Rob D. Mackley
Vanessa Garayburu-Caruso
Vicky L. Freedman
Kristin M. Engbrecht

U.S. DEPARTMENT OF ENERGY

Prepared for the U.S. Department of Energy
under Contract DE-AC05-76RL01830

DISCLAIMER

PACIFIC NORTHWEST NATIONAL LABORATORY
operated by
BATTELLE
for the
UNITED STATES DEPARTMENT OF ENERGY
under Contract DE-AC05-76RL01830

Printed in the United States of America

Available to DOE and DOE contractors from the
Office of Scientific and Technical Information,
P.O. Box 62, Oak Ridge, TN 37831-0062;
ph: (865) 576-8401
fax: (865) 576-5728
email: reports@adonis.osti.gov

Available to the public from the National Technical Information Service
5301 Shawnee Rd., Alexandria, VA 22312
ph: (800) 553-NTIS (6847)
email: orders@ntis.gov <https://www.ntis.gov/about>
Online ordering: http://www.ntis.gov

PNNL-30467

Hydrologic Evaluation of the Ringold Upper Mud Aquifer in the 100-H Area of the Hanford Site

September 2020

Rob D. Mackley
Vanessa Garayburu-Caruso
Vicky L. Freedman
Kristin M. Engbrecht

Prepared for
the U.S. Department of Energy
under Contract DE-AC05-76RL01830

Pacific Northwest National Laboratory
Richland, Washington 99354

Summary

Aquifer tests were recently performed in the Hanford Site 100-H Area to provide a hydrologic evaluation of the Ringold Formation member of Wooded Island – upper mud unit (RUM) aquifer to reduce uncertainty regarding its lateral continuity and characterize aquifer properties within the high-concentration portion of the RUM Cr(VI) plume. A constant-rate pumping test was performed in well 199-H3-22 in October 2019. Additionally, the hydraulic responses from pump and treat (P&T) shutdown events occurring in June, July, and October 2019 were analyzed for aquifer hydraulic properties.

The results from the constant-rate pumping test indicate that the uppermost RUM aquifer is a semiconfined or leaky-confined aquifer and there is lateral hydraulic connectivity extending large lateral distances across the 100-H Area. They also indicate that the uppermost RUM aquifer hydraulic properties are relatively uniform within an inner region of the 100-H test area. However, aquifer properties estimated from responses in observation wells located in the outer region of the test area are higher in transmissivity (T), storativity (S), and vertical hydraulic conductivity within the confining layer (K'). This suggests that as larger portions of the aquifer are investigated, the presence of heterogeneities and their associated impact on observation well response become more evident. Increases in effective aquifer thickness and/or relatively higher leakage through the RUM confining layer to the unconfined aquifer within the radius of investigation may explain the higher hydraulic property estimates.

Confirming lateral connectivity of the RUM aquifer across the 100-H Area is a new finding and can be used to inform the conceptual site model and numerical models supporting remedy optimization. The aquifer hydraulic properties identified in the high-concentration portion of the Cr(VI) plume can be used as input parameters in predictive analyses investigating the effective radius of influence, the number of extraction wells needed, and the remedial effect P&T extraction wells have on removal of mass or hydraulic control of Cr(VI) within the RUM aquifer. This information is important for identifying the time to cleanup and cost for remediating of the RUM aquifer.

Results from shutdown events involving P&T extraction wells in the RUM aquifer provide an additional method for obtaining estimates of aquifer hydraulic properties, as demonstrated by analyzing the hydraulic responses from three P&T shutdown events. Results from three P&T shutdown events tests were consistent with those from the constant-rate pumping test, demonstrating the applicability of P&T shutdown events to inform aquifer characterization that is less disruptive to P&T operations and offers potential cost savings over traditional constant-rate testing approaches.

P&T wells are shut down periodically for maintenance, repair, or other reasons, and these impart a hydraulic recovery response to the aquifer that can be analyzed using methods similar to constant-rate pumping test, assuming certain conditions are met. Opportunistic analysis of shutdown events that occur for operational maintenance purposes is recommended as an additional hydrologic characterization tool. Additionally, P&T shutdown events could be designed and performed with specific hydrologic test objectives in mind.

Acknowledgments

We thank Inci Demirkanli for her technical review of this report. We thank the entire 100-HR-3 project team and P&T operations staff at CHPRC for their support and collaboration (listed alphabetically): Robert Evans, Travis Hammond, Avrom HaWaaboo, Jason Hulstrom, Kris Ivarson, Dean Neshem, Darrell Newcomer, and Sarah Springer. We acknowledge and appreciate Brent Hicks for quality assurance support, Stephanie Liss for GIS mapping support, and Matt Wilburn for editorial assistance.

This document was prepared by the Deep Vadose Zone – Applied Field Research Initiative at Pacific Northwest National Laboratory. Funding was provided by the U.S. Department of Energy (DOE) Richland Operations Office. Pacific Northwest National Laboratory is operated by Battelle Memorial Institute for the DOE under Contract DE-AC05-76RL01830.

Acronyms and Abbreviations

AWLN	automated water level network
CHPRC	CH2M Hill Plateau Remediation Company
CSM	conceptual site model
EW	extraction well
Hf	Hanford formation
MW	monitoring well
OU	operable unit
P&T	pump and treat
PNNL	Pacific Northwest National Laboratory
RUM	Ringold Formation member of Wooded Island – upper mud unit
Rwie	Ringold Formation member of Wooded Island – unit E
SCADA	supervisory control and data acquisition

Contents

Figures

Tables

1.0 Introduction

Historical operations in the 100-HR-3 Groundwater Operable Unit (OU), located in the northcentral part of the Hanford Site (Figure 1.1), have resulted in the contamination of soil and groundwater with hexavalent chromium (Cr[VI]). Cr(VI) in groundwater is distributed as broad plumes within the unconfined aquifer as well as the underlying semiconfined aquifer within the Ringold Formation member of Wooded Island – upper mud unit (RUM) (DOE/RL-2010-95, Rev. 0). Remediation activities involving groundwater pump and treat (P&T) and excavation of contaminated soil have helped to significantly decrease Cr(VI) concentrations in groundwater and shrink the size of plumes in the unconfined aquifer (Figure 1.2). However, high Cr(VI) concentrations (>100 µg/L) continue to persist above target cleanup levels (48 µg/L) in the underlying RUM aquifer in the Horn (area between 100-D and 100-H) and 100-H areas (Figure 1.3). The highest Cr(VI) concentrations in the HR-3 OU now occur in the uppermost RUM aquifer, with some wells located within 75 meters of the Columbia River shoreline.

The presence of Cr(VI) in the RUM has been recognized for decades (DOE/RL-2010-95, Rev. 0); however, the full spatial extent and fate of the Cr(VI) plume in the RUM aquifer in the 100-H Area is still uncertain (DOE/RL-2017-13, Draft A). For example, the flux of Cr(VI) and interactions between the RUM and the Columbia River and the RUM and the unconfined aquifer have not yet been quantitatively assessed (SGW-60571, Rev. 0). Critical parameters such as groundwater flow direction, gradient, and velocity are uncertain for the RUM aquifer. As noted in the 100-HR-3 Remedial Design/Remedial Action Work Plan (RD/RAWP; DOE/RL-2017-13, Draft A), the successful optimization of the groundwater P&T remediation strategy, required timeframe for cleanup, and the eventual strategy for site closure for the RUM aquifer portion of the 100-HR-3 remedy require a more quantitative understanding of Cr(VI) fate and transport behavior and its interactions with the Columbia River.

The results in this report represent a multi-year integrated approach for advanced characterization executed in coordination with the site contractor to support efforts to quantitatively understand groundwater flow and Cr(VI) transport in the RUM aquifer and potential for discharge to the Columbia River. Outcomes of these hydrologic characterization evaluations include estimates of horizontal and vertical hydraulic conductivity, vertical leakage and exchange between the RUM and the overlying unconfined aquifer, groundwater gradient, flow direction, and velocity for the RUM aquifer in the 100-H Area. This information is critically important for developing accurate and representative conceptual site models (CSMs) and developing accurate groundwater flow and transport simulations necessary to optimize the P&T remedy and determine cleanup timeframes for the RUM aquifer.

1.1 Document Scope

This document presents the results of several aquifer tests, including an analysis of a constant-rate pumping test performed in October 2019 in RUM aquifer well 199-H3-22. The constant-rate pumping test involved monitoring aquifer hydraulic responses to pumping in numerous RUM monitoring wells throughout the 100-H Area at a spatial extent much larger any previous investigation. Additionally, aquifer hydraulic responses to shutdown events in RUM aquifer P&T extraction wells provided “opportunistic” hydrologic tests, which were then analyzed for aquifer hydraulic properties. Three P&T shutdown events involving RUM extraction wells were analyzed and compared to the results from the constant-rate pumping test. The results provide additional estimates of the hydraulic properties for the uppermost RUM aquifer and in 100-H Area, indicating lateral continuity of the RUM aquifer within the 100-H Area.

1.2 Document Organization

Following the introduction of this report, Section 2.0 contains background information including the hydrogeology of the 100-H test area, a summary of the conceptual model for contamination in the RUM aquifer, and a detailed summary of previous hydrologic investigations of the RUM aquifer. Section 3.0 discusses areas of uncertainty for the RUM aquifer that drive the need for additional hydrologic investigations that support site cleanup and closure. The methods and results of the hydrologic evaluation are presented in Section 4.0. Section 5.0 provides an integrated hydrologic discussion of the RUM aquifer based on results from the present study and previous analyses, followed by conclusions summarized in Section 6.0. Supplemental information on the hydrologic evaluations are contained in figures provided in Appendix A.

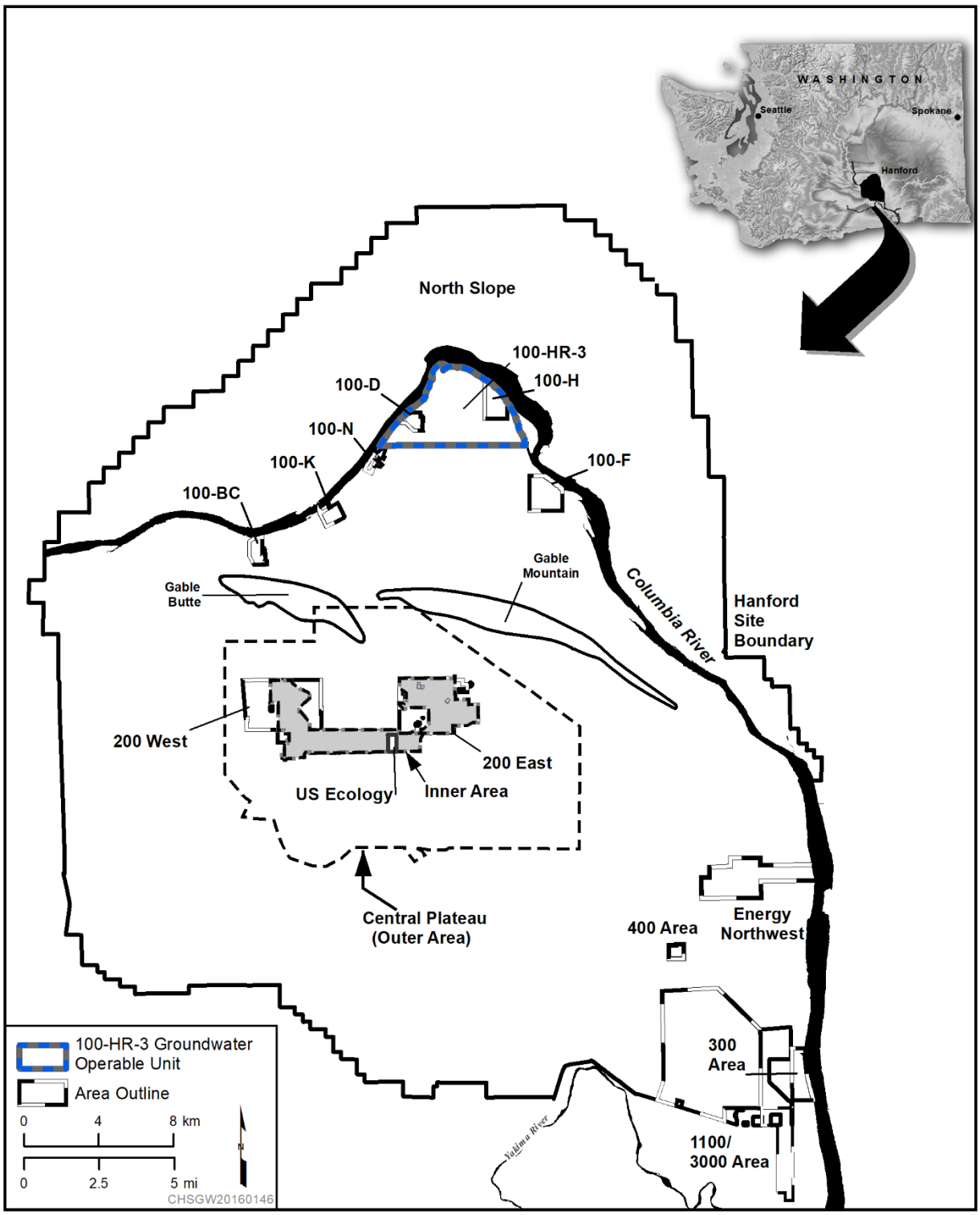

Figure 1.1. Map showing the 100-HR-3 Groundwater Operable Unit located within the northwest region of the Hanford Site (from SGW-60571, Rev. 0).

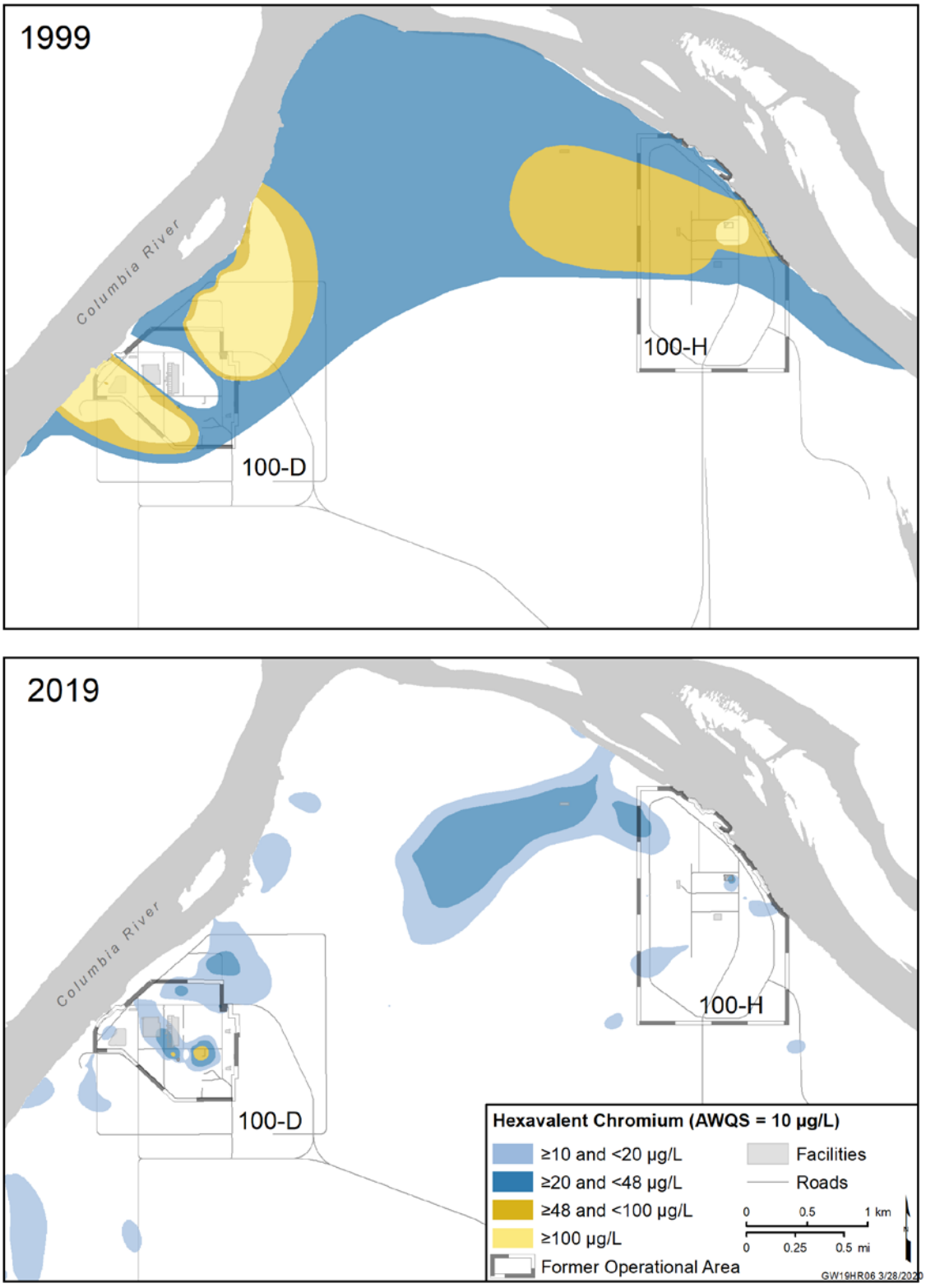

Figure 1.2. Maps showing the decrease in concentration and size of Cr(VI) plumes within the unconfined aquifer in 100-HR-3 from 1999 (upper) to 2019 (lower) as a result of groundwater remediation activities (from DOE-RL-2019-66, Rev. 0).

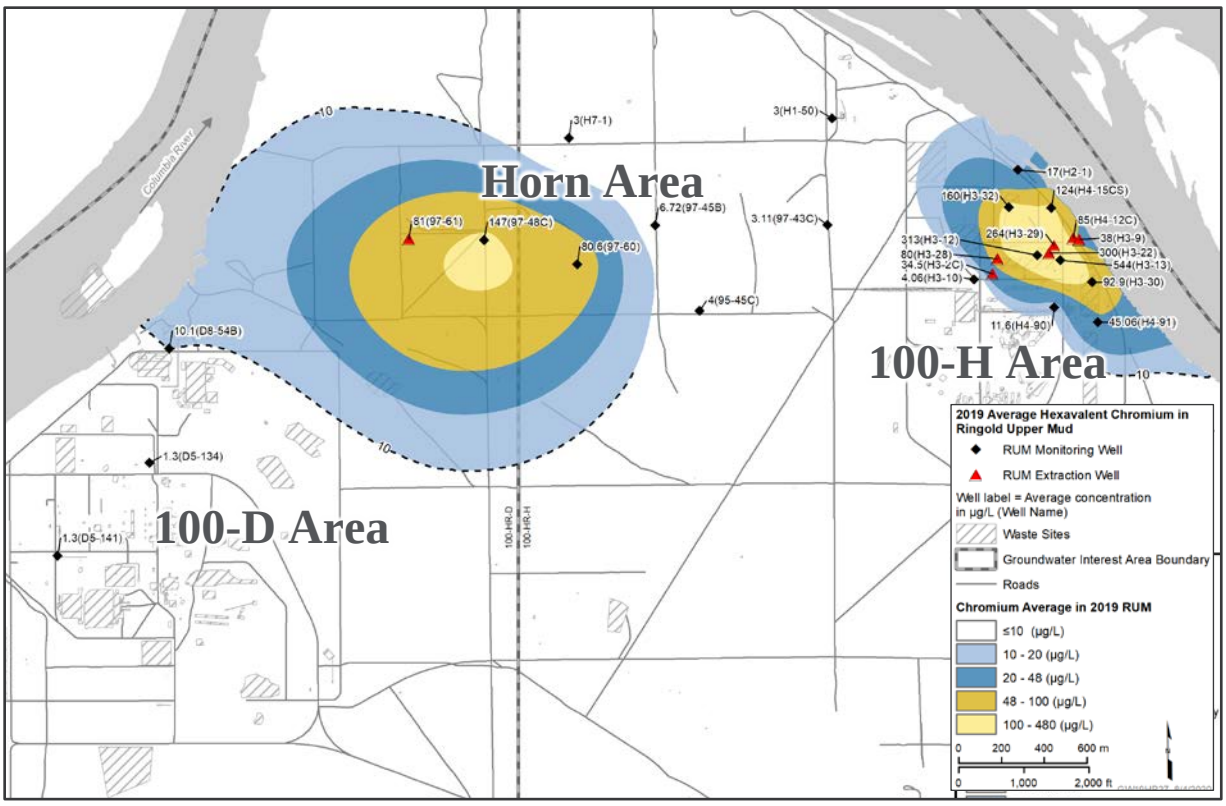

Figure 1.3. Map showing the Cr(VI) plumes in the Horn and 100-H areas within the uppermost RUM aquifer which continue to persist above the 48 µg/L cleanup level (modified from DOE-RL-2019-66, Rev. 0).

2.0 Background

This section provides a summary of the hydrogeology of the test area, conceptual model for contamination in the RUM, previous aquifer hydraulic property investigations, and the emerging needs and data gaps that present risk factors for optimizing groundwater remediation of Cr(VI) in the RUM aquifer.

2.1 100-H Area Hydrogeology

The three hydrogeologic units of interest within the 100-H study area are the Hanford formation (Hf), Ringold Formation member of Wooded Island – unit E (Rwie), and Ringold Formation member of Wooded Island – upper mud unit (RUM) (Figure 2.1; Table 2.1). Material of the Hf (an informal geologic unit) consists predominantly of unconsolidated sediments that cover a wide range of grain sizes, from boulder-sized gravel to sand, silty sand, and silt. The unconfined aquifer at 100-H is primarily within the gravel-dominated Hf, although there are localized areas where the Rwie is present and underlies the Hf (DOE/RL-2010-95). The Rwie unit consists of fluvial matrix supported by gravels and sands with intercalated fine- to coarse-grained sand and silt layers and is relatively less transmissive than the overlying Hf (SGW-60571).

RUM sediments are relatively lower in permeability and form the base of the unconfined aquifer in 100-H Area (Figure 2.1; Table 2.1). The silt- and clay-laden RUM has lower hydraulic conductivity relative to the Hf and Rwie. The top of the RUM forms a confining layer or aquitard between the overlying unconfined aquifer and the uppermost RUM aquifer and varies in thickness from about 3 to 13 meters in the 100-H Area (Table 2.2). Below the fine-grained and low-permeability RUM confining layer is the uppermost RUM aquifer, also referred to as the first water-bearing unit in the RUM (DOE/RL-2010-95). The uppermost RUM aquifer consists of silty-sand layers. Information from additional characterization boreholes drilled recently and hydraulic testing suggests that the uppermost RUM aquifer may be continuous within the 100-H Area up to hundreds of meters laterally (SGW-60571). However, the continuity of the RUM within the entire 100-HR-3 OU and regionally remains uncertain. In the 100-H Area, it appears the uppermost RUM aquifer varies in thickness between about 6 and 14 meters (Table 2.2).

Fine-grained silts and clays form the base of the uppermost RUM aquifer. Deeper transmissive water-bearing units can be found in the RUM (e.g., second and third water-bearing units of the RUM; DOE/RL-2010-95). However, no Cr(VI) contamination has been found in the deeper water-bearing units, and it is highly uncertain if they are laterally continuous and how they relate stratigraphically to other Ringold Formation units regionally.

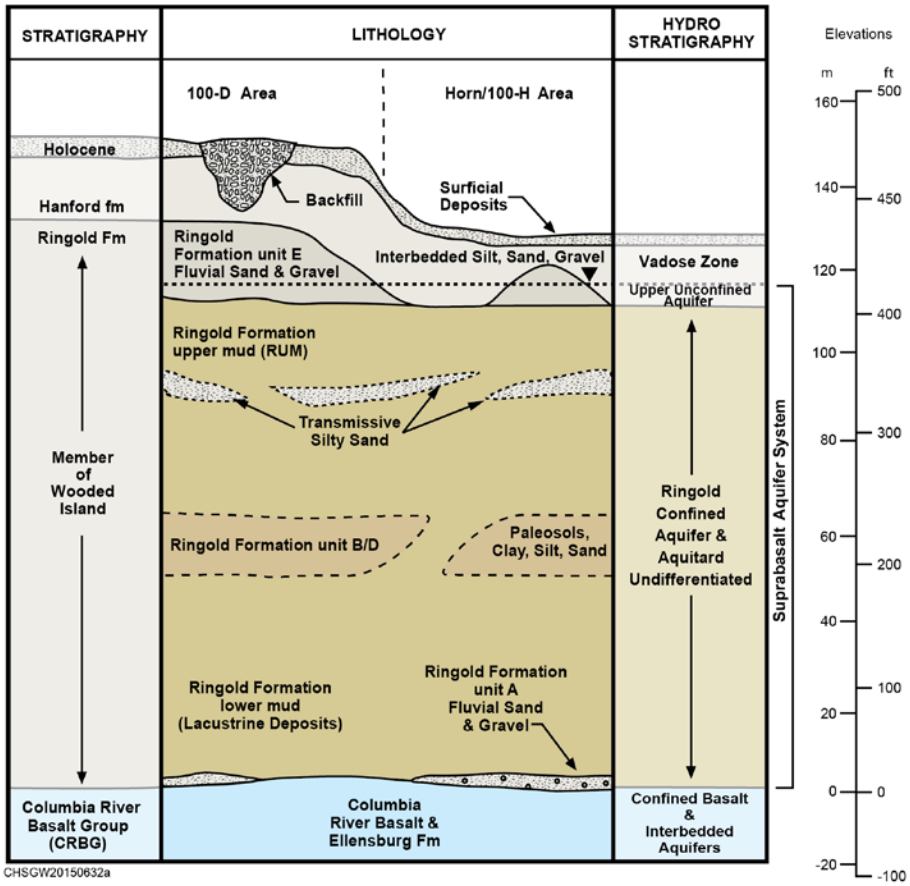

Figure 2.1. Conceptualized hydrogeology for the 100-HR-3 OU (from DOE-RL-2019-66, Rev. 0).

Table 2.1. Elevations of Hydrogeologic Units of Interest for RUM Wells within the 100-H Test Area (shown on the map in Figure 4.1).

Well Name	Hanford Well ID	Ground Surface (elev m)[(a)]	Top of Hf (elev m)	Top of Rwie (elev m)	Top of RUM Aquitard (elev m)	Top of Uppermost RUM Aquifer (elev m)	Base of Uppermost RUM Aquifer (elev m)
199-H2-1	C7631	124.06	124.06	NP	111.87	106.01	92.35
199-H3-10	C7640	129.01	129.01	NP	112.25	98.89	86.00
199-H3-12	C9987	131.62	131.62	NP	114.86	106.76	96.56
199-H3-13	C9989	129.35	129.35	NP	115.33	107.66	95.82
199-H3-22	C9924	129.65	129.65	NP	115.02	106.68	96.97
199-H3-28	C9715	129.99	129.99	119.32	112.01	102.97	95.51
199-H3-29	C9716	129.06	129.06	118.39	115.25	104.68	98.56
199-H3-2C	A4613	128.02	128.02	NP	108.51	97.58	88.34
199-H3-30	C9717	127.82	127.82	NP	114.10	108.93	ND
199-H3-31[(b)]	C9723	128.60	128.60	NP	110.93	107.24	ND
199-H3-32	C9724	128.86	128.86	NP	115.45	109.03	97.80
199-H3-9	C7639	127.01	127.01	NP	111.77	103.87	97.31
199-H4-12C	A4618	126.46	126.46	NP	111.22	102.27	96.11
199-H4-15C[(c)]	A5689	124.63	124.63	NP	110.61	100.12	91.10
199-H4-91	C8788	128.90	128.90	NP	111.68	108.41	ND
199-H4-94[(b)]	C9932	127.70	127.70	112.56	111.01	107.72	94.21

Hf = Hanford formation; Rwie = Ringold Formation member of Wooded Island – unit E; RUM = Ringold Formation member of Wooded Island – upper mud unit

NP = not present; ND = not determined

(a) Elevations for the ground surface and hydrogeologic units are from a pending version of the HR-3 specific Geologic Framework Model; (CP-65222 Rev 0), as communicated from Sarah Springer [CH2M Hill Plateau Remediation Company (CHPRC)] to Rob Mackley (PNNL) on 8/25/2020. Well 199-H4-90 was not included in the hydrogeologic unit information dataset obtained from CHPRC.

(b) Wells 199-H3-31 and 199-H4-94 were drilled and completed in 2020 after the hydrologic testing described in this investigation was performed; however, they are included since they provide additional hydrogeologic information for the test area.

(c) Well 199-H4-15C is host to four piezometers. The piezometer completed in the RUM is 199-H4-15CS.

Table 2.2. Thickness of Hydrogeologic Units of Interest for RUM Wells within the 100-H Test Area (Shown on the Map in Figure 4.1).

Well Name	Hanford Well ID	Hf Thickness[(a)] (m)	Rwie Thickness (m)	RUM Aquitard Thickness (m)	Uppermost RUM Aquifer Thickness (m)
199-H2-1	C7631	12.19	NP	5.86	13.66
199-H3-10	C7640	16.76	NP	13.36	12.89
199-H3-12	C9987	16.76	NP	8.10	10.20
199-H3-13	C9989	14.02	NP	7.67	11.84
199-H3-22	C9924	14.63	NP	8.34	9.71
199-H3-28	C9715	10.67	7.31	9.04	7.46
199-H3-29	C9716	10.67	3.14	10.57	6.12
199-H3-2C	A4613	19.51	NP	10.93	9.24
199-H3-30	C9717	13.72	NP	5.17	ND
199-H3-31[(b)]	C9723	17.67	NP	3.69	ND
199-H3-32	C9724	13.41	NP	6.42	11.23
199-H3-9	C7639	15.24	NP	7.90	6.56
199-H4-12C	A4618	15.24	NP	8.95	6.16
199-H4-15C[(c)]	A5689	14.02	NP	10.49	9.02
199-H4-91	C8788	17.22	NP	3.27	ND
199-H4-94[(b)]	C9932	15.14	1.55	3.29	13.51
	Average[(d)]	***14.8***	***4.0***	***7.7***	***9.8***

Hf = Hanford formation; Rwie = Ringold Formation member of Wooded Island – unit E; RUM = Ringold Formation member of Wooded Island – upper mud unit
NP = not present; ND = not determined

(a) Thicknesses were calculated as the difference in elevation between the top of a selected unit and the underlying unit.
(b) Wells 199-H3-31 and 199-H4-94 were drilled and completed in 2020 after the hydrologic testing described in this investigation was performed; however, they are included since they provide additional hydrogeologic information for the test area.
(c) Well 199-H4-15C is host to four piezometers. The piezometer completed in the RUM is 199-H4-15CS.
(d) Averages are rounded to the nearest tenth of a meter and exclude non-numeric values where units are NP or ND.

2.2 Conceptual Model for Contamination in the RUM

During historical operations of the D, DR, and H reactors (1944-1967; DOE/RL-2010-95), sodium dichromate dihydrate was added to the cooling water as a rust inhibitor for the reactors (DOE/RL-2010-95). Effluent cooling water containing Cr(VI) was discharged to retention basins after passing through the reactors and then released to the Columbia River. Contaminated cooling water leaked from retention basins and discharge of radiologically-contaminated cooling water to the ground and unconfined aquifer resulted in large plumes of Cr(VI) within the unconfined aquifer at 100-HR-3 OU (DOE/RL-2010-95).

The prevailing CSM states that Cr(VI) contamination in the RUM aquifer results from downward migration of the contamination from the overlying unconfined aquifer (SGW-60571; DOE/RL-2010-95). Potential migration pathways are theorized to occur where the clay-silt layer that makes up the top portion

of the RUM unit is thin or absent. During the reactor operations, there were intentional discharges of reactor effluent cooling water to the vadose zone, which resulted in significant vertical mounding of the water table in the 100-D and 100-H Areas (DOE/RL-2010-95). The high hydraulic-head conditions imposed by this mounding could have driven contaminated groundwater downward into the RUM aquifer through hydraulic communication pathways. The lateral continuity, thickness, lithology, and hydraulic properties (e.g., vertical hydraulic conductivity) of the RUM confining layer in the 100-HR-3 OU remain an uncertainty.

2.3 Previous RUM Hydrologic Studies

The uppermost RUM aquifer has been the subject of field hydrologic investigations for decades as remediation of Cr(VI) is an increasing priority. Results from previous 100-H Area aquifer investigations, including results from slug and pumping tests, are reviewed below. The level of detail included in the following is intended to provide a consolidated summary of the testing locations, field methods, and analysis approach associated with reported aquifer hydraulic properties.

2.3.1 Slug Tests

A series of slug tests were performed in wells with screens completed in the uppermost RUM aquifer in the 100-HR-3 OU in 2012 during remedial investigations (DOE/RL-2010-95). At each test well location, three slug withdrawal tests were performed using slugging rods of varying volume and initial displacement, and data were analyzed using the Kansas Geological Survey (KGS) model of Hyder et al. (1994). RUM wells slug tested in the 100-H Area included 199-H3-10, 199-H3-9, and 199-H2-1. Hydraulic conductivity (K) estimates from slug testing results range from 0.6 to 2.0 m/day (Table 2.3), which are noticeably lower than those estimated from pumping tests.

2.3.2 Pumping Tests

PNL-6468 reports results from aquifer tests in RUM wells 199-H3-2C and 199-H4-12C performed in 1987. No details were provided on the specific types of aquifer tests, duration, or analysis methods. They report separate values for transmissivity (T) for each of two well locations, which a parameter typically estimated from pumping tests, so it can be reasonably inferred that a pumping test was performed. It is not known what aquifer model or assumptions were made during the analysis of the drawdown or recovery data. The reported T estimates range from 55.6 to 130.0 m^2/day (Table 2.3). K estimates were reported to range from 18.3 to 42.7 m/day, based on an assumed aquifer thickness of 3.05 meters (10 feet) equal to the screened interval of the test wells (PNL-6468).

In 2009, constant-rate pumping tests were performed in 100-H Area RUM aquifer wells 199-H3-2C, 199-H4-12C, and 199-H4-15CS (SGW-47776). Wells 199-H3-2C and 199-H4-12C were pumped for an extended time period of 43 days and well 199-H4-15CS was pumped for 24 hours. The primary objective of these tests was to identify possible hydraulic communication between the RUM and unconfined aquifers. There were only a few wells completed in the RUM aquifer in 2009 when these tests were performed, which limited the ability to observe RUM aquifer responses away from the pumping well and confirm lateral continuity of the uppermost RUM aquifer. While pumping in well 199-H3-2C, drawdown in unconfined aquifer wells 199-H3-2A and 199-H3-2B was observed and interpreted to indicate hydraulic communication between the two aquifers vertically (SGW-47776). The drawdown and recovery responses in the three RUM pumping wells were analyzed separately using the Cooper-Jacob (1946) straight-line approximation method. Reported T estimates from the three wells ranged from 38.3 to 72.3 m^2/day (Table 2.3), which is slightly lower than the values estimated in the 1987 tests (PNL-6468).

Extensive RUM aquifer testing was performed in 2016. A series of well performance and aquifer tests were performed in uppermost RUM aquifer wells distributed across the 100-H Area (SGW-60571). By 2015, more wells were constructed in the RUM aquifer, which made it more possible to evaluate the lateral continuity of the RUM aquifer. Constant-rate pumping tests (24-hour duration) were performed in RUM wells 199-H3-2C, 199-H3-10, 199-H4-90, and 199-H3-9, while observing aquifer responses to pumping in nearby RUM and unconfined aquifer wells. The drawdown and drawdown derivative data from observation wells, located up to 90 meters away from the pumping well, were analyzed according to the Hantush and Jacob (1955) leaky-confined (without aquitard storage) aquifer model. Leaky-confined aquifer conditions were distinguished based on a distinctive arcuate, downward-trending derivative pattern. Reported transmissivity estimates for the uppermost RUM aquifer ranged from 16.3 to 71.2 m^2/day (Table 2.3). Reported K estimates were calculated using an inferred aquifer thickness (b) value of 3.05 meters (equal to the length of the screened interval), ranging in value from 5.4 to 23.6 m/day (Table 2.3). The 2016 pumping tests also provided the estimates of storativity (S) for the RUM aquifer, and vertical hydraulic conductivity of the RUM aquitard (K') (Table 2.3). Unlike the 2009 testing, no response to unconfined aquifer wells was observed while pumping in RUM aquifer well 199-H3-2C. This may have been due to the much shorter pumping duration in 2016 (24 hours) compared to 2009 (43 days).

Table 2.3. RUM Aquifer Properties Reported in Previous Hydrologic Investigations.

RUM Aquifer Well	Year Tested	Source Reference	Aquifer Test & Analysis Method	T (m^2/day)[a]	K (m/day)	S	K' (m/day)
199-H3-2C	1987	PNL-6468	Pumping test in well 199-H3-2C[b]	55.7	18.3	NR	NR
	2009	SGW-47776	43-day duration pumping test well 199-H3-2C[c]	38.3	NR	NR	NR
	2016	SGW-60571	24-h duration pumping test in well 199-H3-10[d]	71.9	23.6	3.0e-4	5.3e-3
199-H4-12C	1987	PNL-6468	Pumping test in well 199-H4-12C[b]	130.1	42.7	NR	NR
	2009	SGW-47776	43-day duration pumping test in well 199-H4-12C[c]	54.2	NR	NR	NR
	2016	SGW-60571	24-h duration pumping test in well 199-H3-9[d]	16.3	5.4	3.2e-4	3.0e-2
199-H4-15CS	2009	SGW-47776	5.8-h duration pumping test in same well[c]	72.3	NR	NR	NR
199-H3-10	2012	DOE/RL-2010-95	Slug test[e]	NR	1.6	NR	NR
	2016	SGW-60571	24-h duration pumping test in well 199-H3-2C[d]	67.7	22.2	2.1e-4	2.9e-3
199-H3-9	2012	DOE/RL-2010-95	Slug test[e]	NR	0.6	NR	NR
199-H2-1	2012	DOE/RL-2010-95	Slug test[e]	NR	2.0	NR	NR

T = transmissivity of the RUM aquifer (T = K/b)
K = hydraulic conductivity of the RUM aquifer
S = storativity of the RUM aquifer
b = thickness of the RUM aquifer
K' = vertical hydraulic conductivity of the RUM aquitard (confining layer)
NR = not reported

(a) T and K were originally reported in ft^2/day and ft/day, respectively, in PNL-6468, SGW-47776, and DOE/RL-2010-95. Values were converted using a conversion factor of 0.3048 m/ft and rounded to the nearest tenth of a m^2 or m.

(b) No details for the aquifer test type, duration, and analysis methods used in the 1987 testing were provided in PNL-6468. It is inferred that single-well pumping tests were performed separately in the two wells since transmissivity (T) was reported. Reported K estimates were calculated using an aquifer thickness (b) value of 3.05 m (equal to the length of the screened interval).

(c) For the 2009 tests, the drawdown and recovery data from the pumping well during constant-rate pumping tests were analyzed using a Cooper-Jacob (1946) straight-line approximation method which assumes non-leaky and infinite-acting confined aquifer conditions. Due to data quality issues with the recovery data, the estimates from the drawdown data were considered "best estimates" according to SGW-47776 and are included here (estimates from recovery data are omitted). No K estimates were reported.

(d) For the 2016 tests, the drawdown data from observation wells during constant-rate pumping tests were analyzed according to the Hantush and Jacob (1955) leaky-confined (without aquitard storage) aquifer model. Constant-head river boundary effects on the aquifer response were considered. Reported K estimates were calculated using an inferred aquifer thickness (b) value of 3.05 m (equal to the length of the screened interval).

(e) Slug tests were performed in the completed well. Three slug withdrawal tests per test well were performed using slugging rods of varying volume and initial displacement, and data were analyzed using the Kansas Geological Survey (KGS) model of Hyder et al. (1994).

3.0 RUM Aquifer Characterization

Results from previous RUM aquifer investigations have provided a range of hydraulic and storage properties for the uppermost RUM aquifer in several locations within the 100-H Area. They also suggest there is hydraulic communication between the RUM aquifer and the overlying unconfined aquifer and indicate the uppermost RUM aquifer exhibits leaky-confined conditions. However, there are notable areas of uncertainty, discussed below, that need to be addressed to optimize current cleanup operations and reach targeted dates for site closure.

3.1.1 RUM Lateral Continuity

The lateral continuity of the transmissive or water-bearing units in the RUM has been a persistent area of uncertainty and subject of investigation for decades (DOE/RL-2010-95; SGW-60571). It is noted that the designation of these as discrete water-bearing units (and not an *aquifer*) in previous hydrogeologic discussions is likely due to the legacy of uncertainty regarding lateral continuity. Information from numerous boreholes and wells drilled into the RUM in the last decade has helped reduce this uncertainty. In particular, the uppermost or first water-bearing unit in the RUM is identified at generally similar elevations and thicknesses throughout the 100-H Area (Table 2.2). Aquifer pumping tests performed during 2016 in several 100-H Area test areas definitively characterized semiconfined or leaky-confined aquifer conditions for the first water-bearing unit and identified lateral continuity across distances of at least 90 meters and suggested it may extend beyond several hundred meters (SGW-60571). The first water-bearing unit of the RUM was referred to as the *uppermost RUM aquifer* for the first time in SGW-60571, which is consistent with and supported by Freeze and Cherry's (1979) definition of an aquifer as, "a saturated permeable geological unit that can transmit significant quantities of water under ordinary hydraulic gradients."

The results and conclusions from the 2016 RUM testing reported in SGW-60571 were significant in advancing an understanding of the uppermost RUM aquifer. However, results were limited to responses in two test areas located on the western and eastern margins of the 100-H Area. These results did not resolve the uncertainty regarding the lateral continuity of the uppermost RUM aquifer across the entire 100-H Area, the spatial scale of interest to the Cr(VI) plume, and the groundwater P&T remedy in the RUM.

A number of new RUM aquifer wells have been drilled and completed in the central portion of the 100-H Area, and they are located in an intermediate or transitional location relative to the two areas tested in 2016. Pumping from one of the new wells in this central location in the 100-H Area (e.g., well 199-H3-22), while observing aquifer responses in the many RUM wells located throughout the 100-Area in all directions, is an ideal testing scenario to evaluate large-scale lateral continuity.

3.1.2 RUM Aquifer Properties in the High-Concentration Area of the Cr(VI) Plume

The highest Cr(VI) concentrations within the RUM aquifer are located in the central portion of the 100-H Area (Figure 1.3). RUM extraction wells 199-H3-22 and 199-H3-29 and RUM monitoring wells 199-H3-12 and 199-H3-13 are located in this region and had the highest average Cr(VI) concentrations in HR-3 in 2019, with values of 300, 264, 313, and 544 µg/L, respectively (Figure 1.3; DOE/RL-2019-66). Aquifer hydraulic properties have not yet been determined for these new wells and additional aquifer testing is needed to fill this critical information gap. These data serve as inputs for groundwater flow and contaminant transport models that are used for optimizing P&T operations, establishing cleanup

timeframes, and quantifying Cr(VI) flux from RUM. These models require accurate aquifer hydraulic properties throughout the modeling domain, but particularly in this high Cr(VI) focus area.

3.1.3 Opportunistic Analysis of P&T Shutdown Events

The 100-H Area has an active P&T treat remedy in place for mass removal and hydraulic control of Cr(VI), with six extraction wells located in the RUM aquifer (Figure 1.3). Planned and unplanned outages in RUM extraction wells occur periodically (DOE/RL-2019-67). These are referred to as P&T shutdown events and typically involve a stoppage of pumping in one or more RUM extraction wells and impart an observable aquifer recovery response in nearby RUM wells (Spane 2010). Analysis of these P&T shutdown events provides additional opportunities to evaluate aquifer hydraulic properties with no additional field-testing costs. An approach for analyzing P&T shutdown response needs to be demonstrated and compared to results from more traditional or controlled aquifer pumping tests (e.g., constant-rate test).

4.0 Hydrologic Evaluation

This section describes the field-testing methods and corresponding analyses intended to evaluate aquifer hydraulic properties and lateral continuity of the RUM aquifer. The hydrologic evaluation is based on an analysis of results from a constant-rate pumping test performed in well 199-H3-22 and three P&T shutdown events in the 100-H area during 2019.

4.1 Constant-Rate Pumping Test in Well 199-H3-22

A constant-rate pumping test was performed in well 199-H3-22 in October 2019. This well was recently drilled and connected to the 100-HX P&T facility as an extraction well in the higher-concentration portion of the Cr(VI) plume in the RUM (DOE/RL-2019-66; DOE/RL-2019-67). Using an existing P&T extraction well as the stress well in the pumping tests eliminated the need to install a temporary pump and avoided costs and logistical challenges associated with disposing of large volumes of purge water. Test design elements and monitoring information are provided below.

4.1.1 Pre-test Conditions

The six P&T extraction wells in the RUM aquifer in the 100-H test area (199-H3-9, 199-H3-2C, 199-H3-22, 199-H3-28, 199-H3-29, and 199-H4-12C) were shut down about 4 days (94 hours) prior to the start of the constant-rate pumping test to allow the aquifer to recover to ambient conditions (Table 4.1). Subsequent analysis of the recovery responses from the shutdown (see Section 4.2.3) indicate the RUM aquifer water levels equilibrated to static conditions within about 24 hours.

Table 4.1. Sequence of October 2019 RUM Aquifer Testing Activities

Date-Time (PST)	Event	Description
10/10/2019 13:00	Shutdown of all RUM P&T extraction wells in the 100-H Area	Pre-test shutdown of all extraction wells to allow RUM aquifer to recover to static ambient conditions prior to initiation of constant-rate test.
10/14/2019 11:00	Start of drawdown phase of constant-rate pumping test in well 199-H3-22	Flow rate in pumping well set to 129 L/min (34 gpm). All other RUM P&T extraction wells remained off. P&T extraction wells in unconfined aquifer set to stable and near-constant flow rates to minimize potential interference. Duration of the drawdown phase of the test = 24.0 hours.
10/15/2019 11:00	End of drawdown phase and beginning of recovery phase of constant-rate pumping test in well 199-H3-22	All other RUM P&T extractions wells continued to remain off and RUM aquifer was allowed to recover from pumping test for a duration of 45.3 hours.
10/17/2019 08:15	End of recovery phase of constant-rate pumping test in well 199-H3-22	All RUM P&T extraction wells turned back on and resume normal operations.

PST = Pacific Standard Time

4.1.2 Field Testing and Monitoring Configuration

The constant-rate pumping test in well 199-H3-22 was designed to evaluate aquifer hydraulic properties and investigate the lateral continuity of the RUM aquifer across the 100-H Area at spatial scales larger than previously investigated. The pumping well 199-H3-22 is strategically surrounded by RUM aquifer wells, which range in radial distances from 44 to 418 meters (Figure 4.1; Table 4.2).

Pumping flow rates in the P&T wells, such as the constant-rate pumping stress well (199-H3-22), are recorded by the supervisory control and data acquisition (SCADA) system and the recording frequency is variable. Generally, more measurements are recorded during dynamic conditions related to changes in flow rates. These data were obtained from the P&T operations organization through email correspondence.[1] For the constant-rate pumping test, well 199-H3-22 was set to a target flow rate of 129 L/min (34 gpm) using the SCADA system in the 100-HX P&T facility for a pumping duration of 24 hours (Table 4.1). Results from previous RUM aquifer pumping tests indicated that a pumping duration of 24 hours was sufficient to identify RUM aquifer properties at radial distances of hundreds of meters, and that longer pumping durations would likely result in increased constant-head boundary and river-stage effects in the late-time portions of the responses, which complicates the analysis (SGW-60571). After pumping in well 199-H3-22 was stopped, the RUM aquifer was allowed to recover to ambient conditions for a period of 45.3 hours.

The test area includes P&T extraction and injection wells in the unconfined aquifer that operated during the constant-rate test. Extraction and injection flow rates of 100-HX P&T wells operating in the unconfined aquifer near the test area were kept at near-constant values during the testing to minimize any possible interference with the RUM aquifer test observations. An inter-aquifer response was observed previously in a long-duration RUM pumping test performed in 2009 (SGW-47776). However, shorter-duration (24-hour) pumping tests performed in the RUM in 2016 did not indicate inter-aquifer response (SGW-60571). Diurnal fluctuations in the Columbia River stage, which are known to affect water levels in RUM aquifer wells (DOE/RL-2010-95; SGW-60571), occurred during the testing related to typical upstream dam operations. Barometric pressure fluctuations can sometimes also have a discernible impact on well water-level measurements (Rasmussen and Crawford 1997). Where necessary, any non-test-related transients were evaluated and addressed in the analysis.

Pressure monitoring data in the pumping well and observation wells were collected using sensors from a combination of networks. Eight of the RUM wells already had dedicated water-level sensors installed as part of the site-wide automated water level network (AWLN) (Figure 4.1; Table 4.2); however, AWLN data were not available for well 199-H3-30 during the October 2019 test period data for an unknown reason. AWLN data are under configuration and management control by the Hanford Site Soil and Groundwater Contractor. AWLN data were downloaded from the Virtual Library website (http://vlprod.rl.gov/vlib/app/index.cfm). Pacific Northwest National Laboratory (PNNL) sensors were installed in five of the wells in the test area (Table 4.2). For observation wells where AWLN and PNNL data were both available, the PNNL data were used. Comparisons between the PNNL and AWLN monitoring data for the same locations (not shown here) indicated consistent values between the two datasets. Additionally, there were water-level sensors installed in each of the six P&T extraction wells for operation and control purposes (Figure 4.1; Table 4.2) and these data were obtained from P&T Operations organization through email correspondence.[1]

During the constant-rate pumping test, pressures were recorded by the AWLN and PNNL sensors in the observation wells once every second to capture the transient pressure response. The PNNL pressure sensor installed in the pumping well (199-H3-22) recorded measurements once every 2 seconds. The recording frequency of the P&T pressure measurements is set by the P&T facility's SCADA system and controlling the recording frequency during the constant-rate test was not possible. During the test, pressures in the P&T wells were recorded by the SCADA system at varying frequencies, ranging from multiple times per second to only once every 2 hours.

[1] P&T flow and level data for HX wells were electronically transmitted through email correspondence from the P&T operations organization to PNNL in two separate batches, one sent on 1/1/2020 and another on 2/12/20.

Table 4.2 contains a summary of information for the network of RUM aquifer wells in the 100-H test area instrumented with pressure sensors and available for monitoring the hydrologic testing. Note that two new RUM aquifer wells, 199-H3-31 and 199-H4-94, were drilled and completed in the 100-H Area in 2020 and were not available to monitor the hydrologic testing activities performed in this evaluation.

4.1.3 Constant-Rate Pumping Test Analysis

The analysis of the results from the October 2019 constant-rate pumping test performed in well 199-H3-22 is a quantitative evaluation of the drawdown and recovery phases of the test as observed in multiple observation wells. The test analysis was conducted in two phases. The first phase focused on identifying the operative aquifer model and presence of any hydrologic boundaries or transient non-test hydraulic effects (e.g., fluctuations in barometric pressure, river-stage changes, or impacts by other 100-HX P&T wells). The subsequent second phase of analysis focused on estimating the aquifer hydraulic and storage properties of the uppermost RUM aquifer and aquitard leakage properties of the intervening RUM confining layer throughout the 100-H test area.

The analysis focused only on responses in the observation wells. The combined effects of partial penetration and well skin (i.e., additional drawdown due to inefficiency of the well rather than the permeability of the aquifer) are less impactful to response in observation wells compared to the pumping wells. Additional drawdown due to the effects of partial well penetration diminish with radial distance from the pumping well (r) and can be ignored at observation well distances ≥1.5 times the aquifer thickness ($r \geq 1.5b$) (Hantush 1962). As noted by Spane (1993), this is valid when certain test-time parameter conditions are met. The radial distance from the pumping well for all observation wells used in this analysis (Table 4.2) are noticeably greater than 1.5 times the average RUM aquifer thickness and meet this requirement for assuming fully-penetrating conditions ($r > 1.5b = 1.5*9.8$ m = 14.7 m).

4.1.3.1 Non-Test-Related Effects

A preliminary evaluation was performed to identify transient hydraulic effects from unconfined aquifer P&T wells near the test area or fluctuations in barometric pressure and river stage on the observed aquifer test drawdown and recovery responses. No interferences from barometric or unconfined aquifer P&T wells were evident in the responses. However, river-stage effects were evident during the late-time periods of the drawdown and recovery phases when plotted on a log-log scale. Where necessary, late-time test response data were excluded from the type-curve matching analyses described below to minimize impacts by river-stage fluctuations on estimated RUM aquifer properties.

Table 4.2. Information for RUM Aquifer Wells for Monitoring of 2019 Hydrologic Testing

Well Name	Well Type[a]	P&T ID[b]	Nominal Diameter (inches)	Easting[c] (m)	Northing (m)	Distance to 199-H3-22[d] (m)	Top of Screen[e] (elev m)	Bottom of Screen (elev m)	Pressure Monitoring Network[f]
199-H3-22	EW	HE11	6	577897.07	152847.99	0.0	106.03	96.88	PNNL & P&T
199-H3-29	EW	HE14	6	577921.46	152884.22	43.7	111.00[g]	101.25	PNNL & P&T
199-H3-12	MW		6	577842.32	152838.62	55.5	103.42	98.85	PNNL & AWLN
199-H3-13	MW		6	577950.58	152815.48	62.6	104.06	96.41	PNNL & AWLN
199-H4-12C	EW	HE10	6	578011.772	152919.812	135.3	104.51	101.47	P&T
199-H3-9	EW	HE13	6	578039.12	152913.6	156.5	103.19	100.15	P&T
199-H3-28	EW	HE12	6	577655.35	152822.58	243.1	102.14	96.04	P&T
199-H3-30	MW		6	578100.23	152712.09	244.4	108.55	102.45	AWLN[h]
199-H4-90	MW		6	577922.94	152592.59	256.7	107.07	102.49	AWLN
199-H3-2C	EW	HE09	6	577632.065	152750.302	282.4	97.54	94.49	P&T
199-H3-32	MW		6	577709.81	153063.5	285.5	102.65	99.60	PNNL & AWLN
199-H3-10	MW		6	577545.14	152723.52	373.3	97.66	94.61	AWLN
199-H4-91	MW		6	578126.58	152524.1	397.0	107.50	102.93	AWLN
199-H2-1	MW		6	577752.31	153239.89	417.8	104.57	101.52	AWLN

(a) Well types include P&T extraction wells (EW), monitoring wells (MW), and piezometers hosted by monitoring wells (MP).
(b) Unique identifier used by the 100-HX P&T facility for extraction wells from DOE/RL-2019-67.
(c) Horizontal coordinates in Washington State Plane South obtained from Environmental Dashboard Application (EDA; https://ehs.chprc.rl.gov/eda/: last accessed on 8/25/2020). The precision of coordinates reported in EDA has been retained here.
(d) Radial distance calculated from the horizontal coordinates and rounded to the nearest tenth of a meter.
(e) Calculated using ground surface elevations and screen depths under management and configuration control by the site contractor (CHPRC). Surface elevations are from a pending version of the HR-3 specific Geologic Framework Model; CP-65222 Rev 0, as communicated from Sarah Springer (CHPRC) to Rob Mackley (PNNL) on 8/25/2020. Screen depths were downloaded from the Environmental Dashboard Application (EDA; https://ehs.chprc.rl.gov/eda/; last accessed on 9/11/2020). Values shown were rounded to the nearest cm.
(f) Pressure monitoring during hydrologic testing was done using a combination of PNNL sensors, sensors in P&T wells, and AWLN sensors.
(g) For well 199-H3-29, there is a blank section of casing from an elevation of 105.82 to 104.30 m that separates two sections of screen.
(h) 199-H3-30 is part of the AWLN, but no data are available during the October 2019 constant-rate pumping test for an unknown reason.

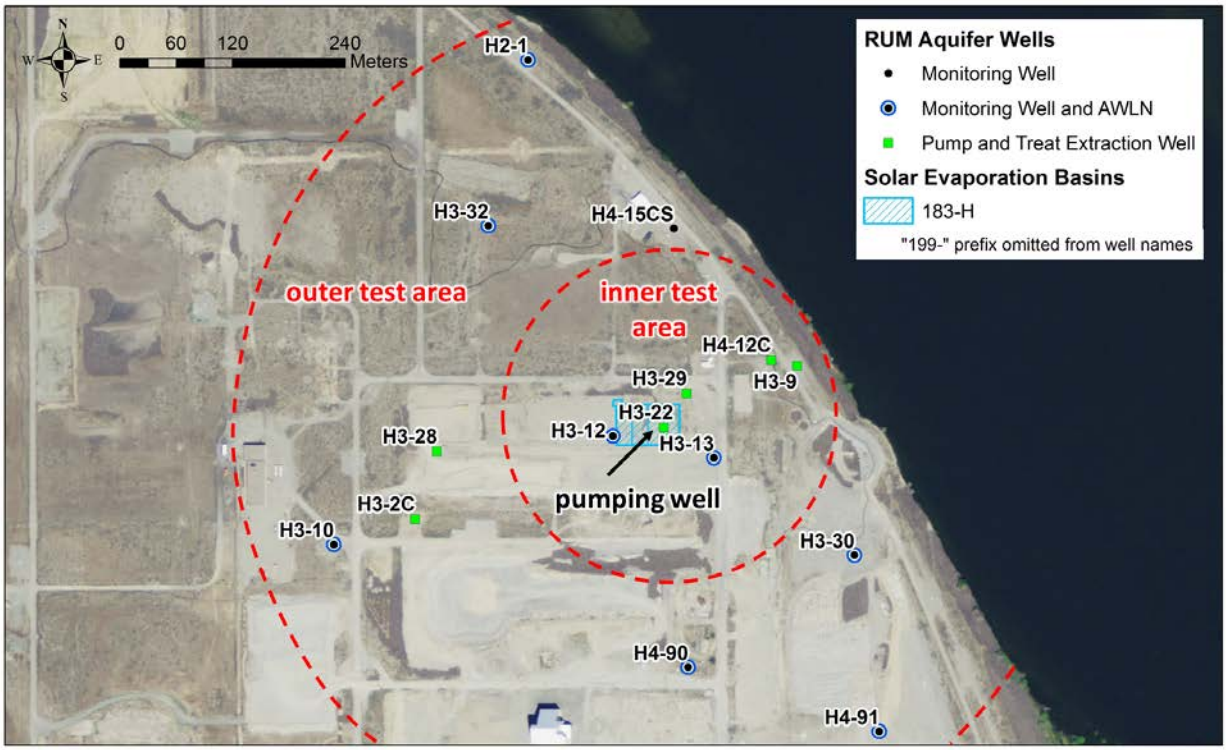

Figure 4.1. Map showing the location of the pumping well and observation wells used in the constant-rate pumping test in well 199-H3-22 in October 2019. Inner and outer regions of the test area are delineated with dashed lines.

4.1.3.2 Diagnostic Evaluation of Operative Aquifer Model

Previous aquifer investigations have identified leaky-confined aquifer conditions for the uppermost RUM aquifer in the 100-H Area (SGW-60571). Although similar conditions were expected, the operative aquifer model exhibited by the RUM was re-evaluated through a diagnostic analysis of log-log plots of drawdown and recovery and their associated derivative patterns from this test in an approach described by Bourdet et al. (1989) and (Spane 1993).

Figure 4.2 shows the drawdown derivative responses plot on a log-log scale for three example observation wells during the constant-rate pumping test. The derivatives exhibit the same arcuate, downward pattern which is characteristic of a leaky-confined aquifer without confining (aquitard) storage (Hantush and Jacob 1955), as shown in Figure 4.3. Note that Figure 4.2 shows there is a scatter and an apparent increase in the derivative values in the late-test time portion of the responses (after about 1000 minutes); this is discussed in more detail in the subsequent section. Increased leakage through the confining layer as represented with the family of "r/B"[1] leakage curves in Figure 4.3 shows earlier stabilization to a lower drawdown value and earlier decrease of the drawdown derivative toward zero. Similar derivative response patterns were observed for the other observation wells. These results are consistent with those from previous RUM aquifer testing (SGW-60571).

[1] The "r/B" leakage curve relationships of Hantush and Jacob (1955) shown in Figure 4.3 are defined by the radial distance from the pumped well, r, divided by the "leakage factor" B, which is equal to the square root of the confined aquifer transmissivity, T, multiplied by the confining layer thickness, b', and divided by the confining layer vertical hydraulic conductivity, K'; $B = (T\ b'/K')^{1/2}$.

It has been previously noted that response patterns resembling that of a leaky aquifer can occur in confined or unconfined conditions (SGW-60571). As discussed by Lohman (1972) and Spane (1993), the selection of the appropriate drawdown type curve should be informed and supported by the hydrogeologic CSM. As discussed in Section 2.2, the CSM for transport of Cr(VI) and other contaminants from the unconfined aquifer downward into the RUM aquifer involves migration though leakage where the intervening RUM confining layer is sufficiently permeable or missing. The diagnostic leaky-confined response exhibited by the drawdown and recovery derivatives is consistent with the RUM CSM.

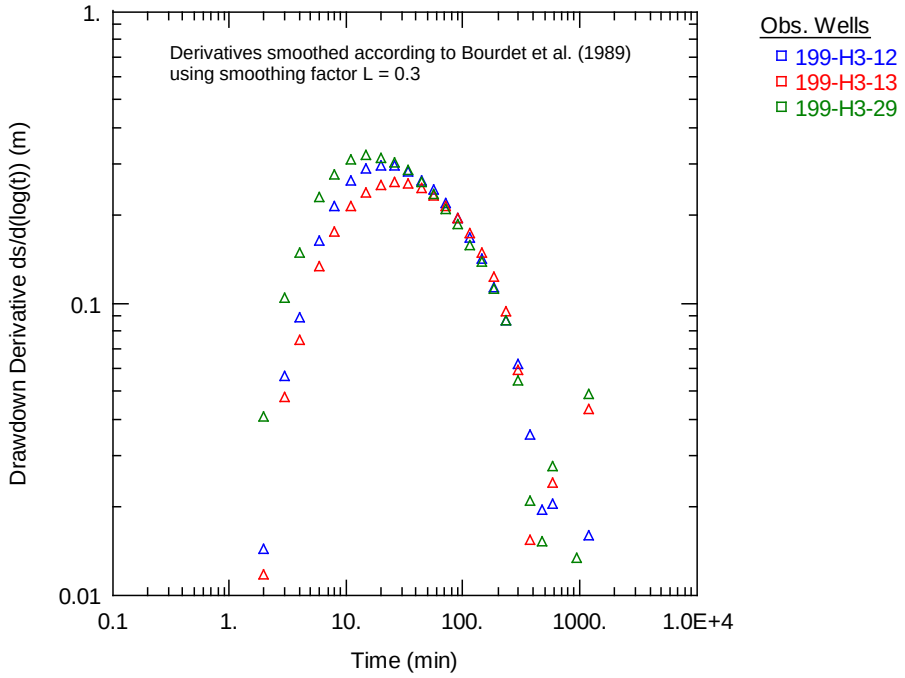

Figure 4.2. Diagnostic log-log plot showing drawdown derivative responses during the constant-rate pumping test in well 199-H3-22.

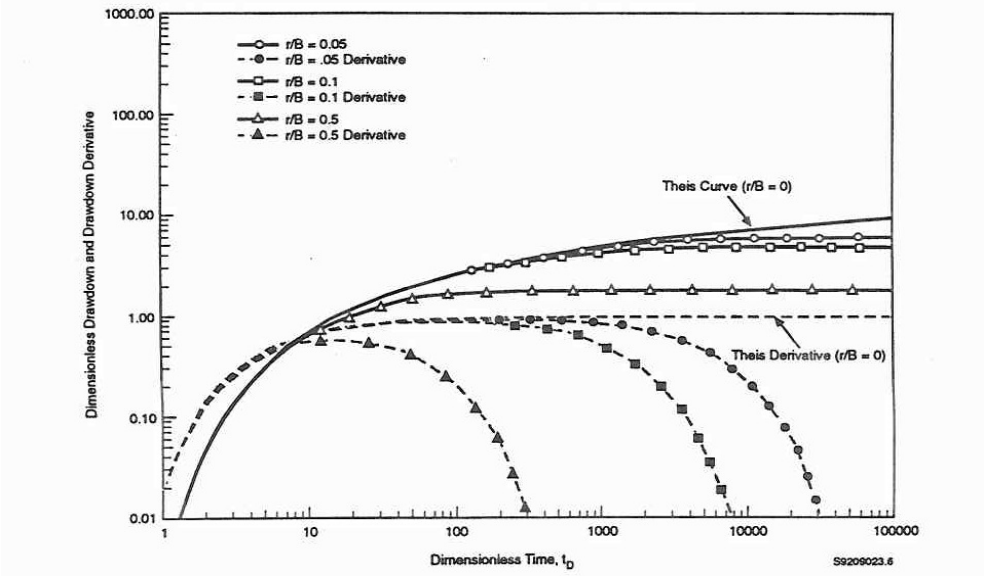

Figure 4.3. Dimensionless drawdown and drawdown derivatives predicted for a constant-rate pumping test in a leaky-confined aquifer, with no confining layer storage, with varying amounts of leakage through the confining layer (r/B = 0.05, 0.1, and 0.5) based on the analytical model of Hantush and Jacob (1955). The fully-confined aquifer model of Theis (1935; r/B = 0) is included for reference (figure from Spane 1993).

4.1.3.3 Type-Curve Matching Analysis

Aquifer properties of the uppermost RUM aquifer and the overlying confining layer were estimated using a type-curve matching analysis of the responses from the constant-rate pumping test in well 199-H3-22. The Hantush and Jacob (1955) leaky-confined aquifer analytical model was used to identify hydraulic properties, as implemented in the AQTESOLV software Version 4.5 (Duffield 2007, 2009). As noted earlier, pressure measurements were recorded at a high temporal frequency (e.g., every second) during the constant-rate testing to capture the transient responses; however, the drawdown and recovery data were filtered to a uniform logarithmic spacing for visual enhancement of the log-log plots during the analysis within AQTESOLV.

In addition to the drawdown data, the pressure response from the recovery phase of the test was analyzed to provide a secondary dataset to evaluate consistency and reproducibility of obtained aquifer properties. Agarwal (1980) developed a method for analyzing recovery data using type-curve methods that were originally developed for analyzing drawdown data. Prior to the type-curve matching analysis, the time values for the recovery data were transformed to an equivalent time (t_e) according to

$$t_e = \frac{t_p * t'}{t_p + t'} \tag{4.1}$$

where:

t_p = total time of pumping during the drawdown phase of the test
t' = elapsed time since pumping stopped

As noted previously, the late-time drawdown and recovery data for some of the observation wells show some river-stage fluctuations. In general, river-stage effects were more evident in the recovery responses. Deviations from the type-curve during the late-time portions of the recovery response were higher in observation wells closer to the river and/or farther away from the pumping wells but are generally less than 0.02 m. These late-time "noisy" data were excluded from the type-matching analysis. Additionally, the first 30 minutes of each test were excluded due to non-ideal startup conditions at the beginning of the drawdown and recovery phases of the test. The pump required 15-20 minutes to stabilize at the targeted flow rate, and backflushing of water back down into the pumping wells occurred for about 15-30 minutes after the pump was turned off.

Table 4.3 summarizes the prescribed parameters used in the type-curve matching analysis. The transmissivity (T), hydraulic conductivity (K = T/b), and storativity (S) of the uppermost RUM aquifer are obtained, along with the confining-layer leakage factor (B) and vertical hydraulic conductivity, through the type-curve matching of the observed responses.

Type-curve matching was performed for each response at a given observation well location individually. An alternative approach is to simultaneously analyze the responses from multiple observation wells together in composite to estimate a single set of properties that describe a laterally uniform or homogeneous aquifer. Individual analysis of the responses provided a large collection of results that indicate the range of hydraulic properties within the test area.

Table 4.3. Analysis Parameters for Constant-Rate Pumping Test in Well 199-H3-22

Parameter	Value(s)	Comments and Basis
Pumping rate (Q)	129 L/min (34 gpm)	Observed flow rate during drawdown phase of test from P&T flow rate data obtained from CHPRC.
Aquifer thickness (b)	9.8 m	Average thickness of the uppermost RUM aquifer within the test area (Table 2.2). *Note the analysis is relatively insensitive to this parameter*.
RUM confining layer (aquitard) thickness (b')	7.7 m	Average thickness of the uppermost RUM aquitard (top confining layer) within the test area (Table 2.2). *Note the analysis is relatively insensitive to this parameter*.
Vertical anisotropy (Kz/Kh)	0.1	Prescribed value representative of layered sediments (Freeze and Cherry 1979). *Note the analysis is relatively insensitive to this parameter*.
Aquifer boundary conditions	Semi-infinite aquifer with a single constant head boundary on eastern side of test area	The constant-head boundary effects of the Columbia River, located approximately 200 meters east of well 199-H3-22, were represented using image well theory (Ferris et al. 1962), as implemented in the AQTESOLV software. Coordinates for river recharge boundary (Washington State Plane South; m): X_1,Y_1 = 578097, 162848 X_2,Y_2 = 578097, 142848
Derivative smoothing factor (L)	0.3	The derivative smoothing method of Bourdet et al. (1989), as implemented in the AQTESOLV software, was used. An L-factor value <0.5 helps to smooth noisy responses without introducing unwanted distortion.
Analytical solution	Hantush and Jacob (1955)	Leaky-confined aquifer model, without aquitard storage, based on derivative analyses and hydrogeologic conceptual model.

4.1.3.4 Constant-Rate Pumping Test Results

Table 4.4 contains the aquifer property estimates from the analyses of the drawdown and recovery responses at each observation well location. Appendix A contains additional log-log plots of the observed drawdown and recovery responses and estimated aquifer properties from the type-curve matching analysis for each observation well location. The drawdown and recovery estimates were averaged together to provide a single estimate at each location, and these location-averaged values are used to simplify the discussion of the results in the following section. Response exhibited in an observation well to pumping is not solely determined by the aquifer properties immediately surrounding that observation well or directly between the observation well and the pumping well (Butler and Liu 1993). This analysis recognizes that the observed response and the associated aquifer property estimate for an individual observation well in this analysis are influenced by properties and conditions within the larger-scale radius of investigation. However, evaluation of the range of estimates between observation wells or diagnostic comparisons of the geometric mean values for the inner and outer regions of the test area were done to help indicate the presence of any non-ideal test conditions, spatial variability, or scale-dependency

Wells 199-H3-12, 199-H3-13, 199-H3-29, 199-H3-9, and 199-H4-12C are located relatively close to the pumping well within an inner region of the test area (Figure 4.1). Figure 4.4 shows the observed responses and estimated aquifer properties from the type-curve matching analysis for well 199-H3-12 as an example. The drawdown and recovery derivatives for all five inner test area wells exhibit the definitive arcuate, downward pattern of a leaky-confined aquifer (without confining layer storage). The similarity in estimated aquifer and confining layer properties for the five wells suggests that the uppermost RUM aquifer and confining layer are relatively uniform within the inner test region. Average aquifer transmissivity (T) estimates are between 43.8 and 62.4 m^2/day in this inner region. Using the average aquifer thickness value (b = of 9.8), the calculated average hydraulic conductivities are estimated between 4.5 and 6.4 m/day. Storativity (S) estimates range between $1.4x10^{-4}$ and $3.1x10^{-4}$. The average vertical hydraulic conductivity (K') estimates for the RUM confining layer vary from $3.6x10^{-3}$ to $6.8x10^{-3}$ m/day within the inner region of the test area.

Table 4.4. Uppermost RUM Aquifer and Confining Layer Hydraulic Property Estimates from October 2019 Constant-Rate Pumping Test in Well 199-H3-22

Region of Test Area	Observation Well (radial distance[a] in m)	Test Phase	T (m^2/day)	K (m/day)	S	K' (m/day)
Inner	199-H3-29 (43.7)	Drawdown	49.1	5.0	1.5E-04	3.7E-03
		Recovery	47.9	4.9	1.4E-04	3.6E-03
		average[b]	***48.5***	***4.9***	***1.4E-04***	***3.6E-03***
	199-H3-12 (55.5)	Drawdown	43.2	4.4	1.5E-04	7.5E-03
		Recovery	44.3	4.5	1.4E-04	6.1E-03
		average	***43.8***	***4.5***	***1.5E-04***	***6.8E-03***
	199-H3-13 (62.6)	Drawdown	46.4	5.0	1.7E-04	3.7E-03
		Recovery	44.5	4.5	1.6E-04	3.8E-03
		average	***45.5***	***4.8***	***1.6E-04***	***3.8E-03***
	199-H4-12C (135.3)	Drawdown	60.8	6.2	3.1E-04	6.4E-03
		Recovery	64.1	6.5	3.1E-04	6.7E-03
		average	***62.4***	***6.4***	***3.1E-04***	***6.6E-03***
	199-H3-9 (156.5)	Drawdown	46.6	4.8	3.4E-04	5.3E-03
		Recovery	56.4	5.8	2.8E-04	6.4E-03
		average	***51.5***	***5.3***	***3.1E-04***	***5.8E-03***
		Geometric Mean[c]	**49.9**	**5.1**	**2.0E-04**	**5.1E-03**
Outer[d]	199-H3-28 (243.1)	Drawdown	144.1	14.7	5.4E-04	1.9E-02
		Recovery	141.8	14.5	5.2E-04	1.8E-02
		average	***143.0***	***14.6***	***5.3E-04***	***1.9E-02***
	199-H4-90 (256.7)	Drawdown	218.2	22.3	1.3E-03	2.5E-02
		Recovery	236.8	24.2	1.0E-03	6.9E-03
		average	***227.5***	***23.2***	***1.2E-03***	***1.6E-02***
	199-H3-2C (282.4)	Drawdown	152.0	15.5	6.0E-04	2.1E-02
		Recovery	140.0	14.3	5.9E-04	1.4E-02
		average	***146.0***	***14.9***	***5.9E-04***	***1.7E-02***
	199-H3-32 (285.5)	Drawdown	196.1	20.0	8.3E-04	4.2E-02
		Recovery	149.1	15.2	5.4E-04	3.2E-02
		average	***172.6***	***17.6***	***6.9E-04***	***3.7E-02***
	199-H3-10 (373.3)	Drawdown	124.3	12.7	6.8E-04	2.7E-02
		Recovery	112.7	11.5	4.2E-04	2.5E-02
		average	***118.5***	***12.1***	***5.5E-04***	***2.6E-02***
		Geometric Mean	**157.6**	**17.0**	**7.3E-04**	**2.5E-02**
Constant-Rate Pumping Test Estimates Combined (n=20)		**Min**	**43.2**	**4.4**	**1.4E-04**	**3.6E-03**
		Max	**236.8**	**24.2**	**1.3E-03**	**4.2E-02**
		Geometric Mean	**88.5**	**9.1**	**3.6E-04**	**1.0E-02**

T = transmissivity of the RUM aquifer (T = K/b)
K = hydraulic conductivity of the RUM aquifer calculated using b = 9.8 m (Table 2.2)
S = storativity of the RUM aquifer
b = thickness of the RUM aquifer
K' = vertical hydraulic conductivity of the RUM aquitard (confining layer)

(a) Radial distances, in meters, from pumping well 199-H3-22 (Table 4.2).
(b) Aquifer properties estimated separately for the drawdown and recovery phases were averaged to provide a single value at each observation well location.
(c) Geometric mean calculated using the average of the drawdown/recovery.
(d) Wells 199-H2-1 and 199-H4-91, located 397.0 and 417.8 m from the pumping well, respectively, did not exhibit observable pressure responses to the test. Additionally, there were no AWLN pressure monitoring data available for well 199-H3-30 during the test period.

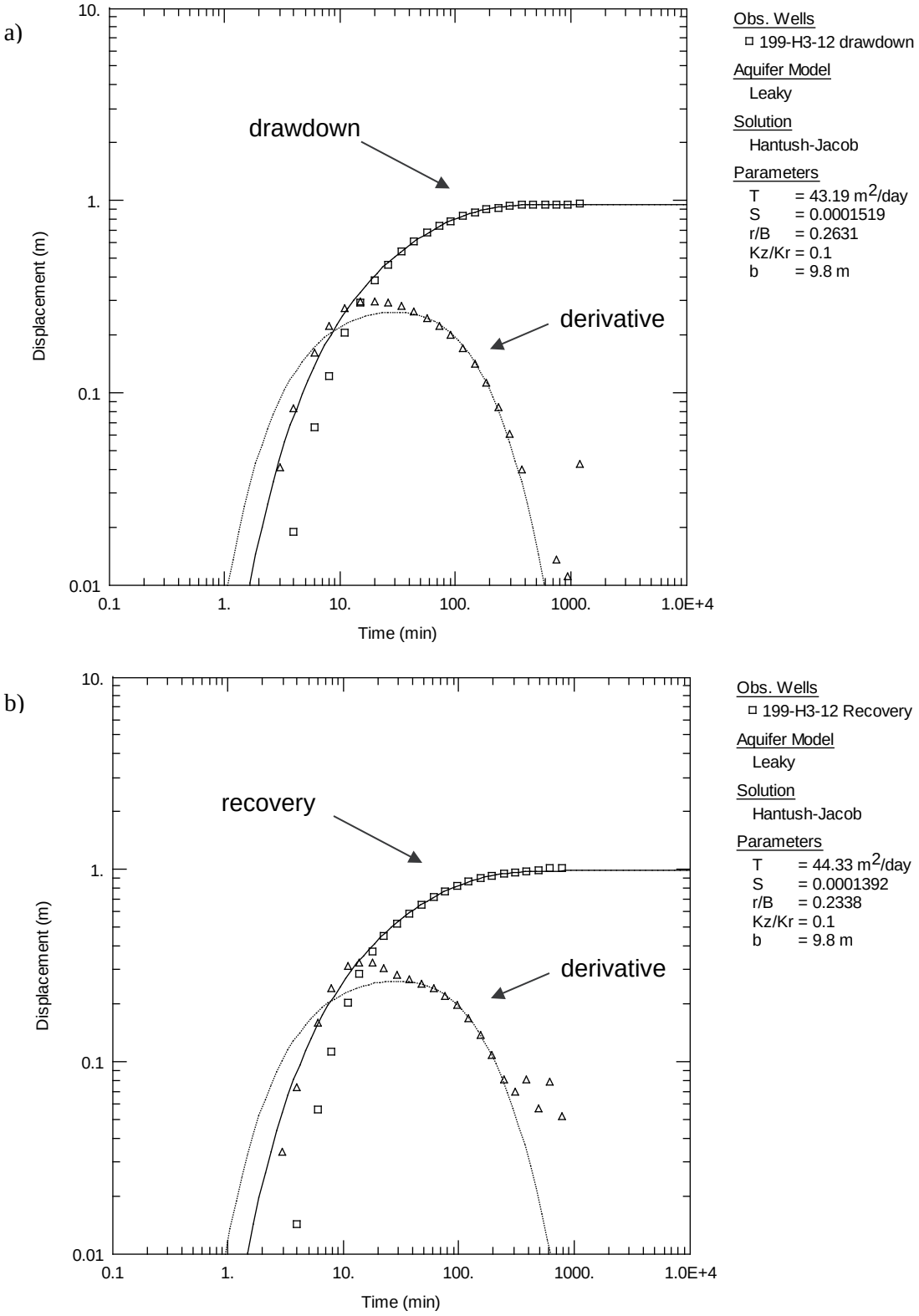

Figure 4.4. Example figure showing type-curve matches to the a) drawdown and b) recovery responses observed for well 199-H3-12 to the constant-rate pumping test in well 199-H3-22.

Responses in the outer test area wells (199-H3-2C, 199-H3-10, 199-H3-28, 199-H3-32, and 199-H4-90) demonstrate spatial variability and lateral heterogeneity observable in the uppermost RUM aquifer when observed at larger radial distances. They show higher overall values of T, K, S, and K' in comparison to the inner region of test wells (Table 4.4). Average T estimates in these three outer-area wells range from 118.5 to 227.5 m^2/day (Table 4.4). Estimates of average S vary between $5.3x10^{-4}$ and $1.2x10^{-3}$. The average K' for the confining layer in the five outer-test area wells ranges from $1.6x10^{-2}$ to $3.7x10^{-2}$ m/day (Table 4.4).

4.2 Opportunistic P&T Shutdown Events

The five groundwater P&T systems in the 100 Area river corridor are designed to operate continuously. In fact, facility run-time percentages in 2019 ranged from 95.2% to 99.6% (DOE/RL-2019-67). However, there are times when wells or groups of P&T wells are turned off temporarily for activities such as facility maintenance, pump replacement, and manual well water-level measurements. These P&T well shutdowns provide an opportunity to evaluate aquifer hydraulic properties obtained through analysis of the observed shutdown-recovery response in nearby wells (Mackley et al. 2020).

Aquifer hydraulic responses from RUM extraction well shutdown events in June, July, and October 2019 were analyzed and compared to results from the controlled constant-rate pumping test in well 199-H3-22 discussed previously. This section briefly discusses the theoretical basis for analyzing P&T shutdown events using an analytical approach similar to the constant-rate pumping tests previously discussed and results obtained from an analysis of three shutdown events that occurred in 2019 in the 100-H test area.

4.2.1 Aquifer Response to P&T Shutdown Events

P&T shutdown events provide an alternative and potentially less-impactful testing approach that can still be performed in settings where there is an active P&T remedy. Conceptually, shutdown tests involve stopping flow to one or more P&T wells (referred to as stress wells), while maintaining flow to the other P&T wells in the test area.

The total composite aquifer response to the shutdown event is a superposition of the impact from surrounding P&T wells (prior to and during the shutdown-recovery test) and the initiation of the shutdown of the stress well(s) (Todd 1980; Spane 2010). Figure 4.5 illustrates an example of a single P&T well shutting down and the associated pressure recovery response in a leaky-confined aquifer. As noted by Spane (2010), the recovery component of the shutdown response can be isolated or de-superposed from the total composite response and analyzed as an equivalent constant-rate pumping test response.

4.2.2 Assumptions and Requirements

As noted above, the total composite response to the shutdown event is a superposition of the recovery response to the shutdown combined with any other input stress to the aquifer occurring before or during the shutdown event. Simplifying assumptions of this analysis included 1) flow to the stress well(s) and other nearby P&T wells has been constant for a sufficient amount of time prior to the shutdown to allow the aquifer to stabilize such that there is little or no background trend, and 2) flow rates are constant to the P&T extraction well(s) that are left running during the shutdown event. This allows the observed pressure recovery response to be attributed solely to the shutdown event and analyzed as an equivalent constant-rate pumping test. The amount of necessary pre-test flow stabilization depends on the site-specific hydrologic conditions. The leaky-confined aquifer conditions allow flow to stabilize relatively quickly (days rather than weeks) to changes in pumping rates, as indicated by the responses from the constant-rate pumping test in well 199-H3-22 (Figure 4.4).

It is also assumed that the recovery response is not affected by other extraneous stresses such as barometric or river-stage fluctuations. Results from the October 2019 constant-rate pumping tests indicate river-stage fluctuations can be seen in the late-time portion of pumping test responses for the uppermost RUM aquifer in the 100-H test area, but the type-curve matching analysis can be restricted to include only the unaffected portion of the response.

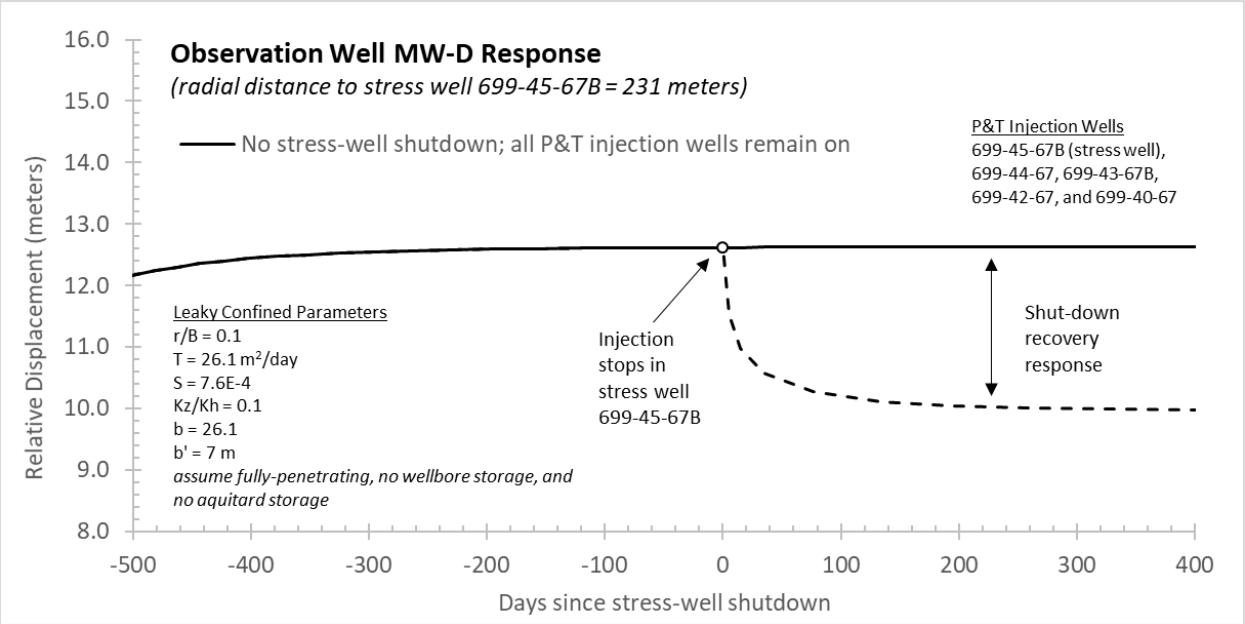

Figure 4.5. Example illustrating a hypothetical P&T shutdown event involving turning off flow to a single "stress" well and the simulated leaky-confined aquifer response (from Mackley et al. 2020).

4.2.3 Multi-Pumping Well Analysis

The recovery components of the shutdown response from each of the three P&T shutdown events were analyzed as equivalent constant-rate pumping tests within AQTESOLV. The same prescribed aquifer properties and leaky-confined analytical solution used in the analysis of the October 2019 constant-rate pumping test were used (Table 4.3).

P&T shutdown events involved stoppage of flow in multiple P&T extraction wells (Table 4.5). The multiple stress wells were incorporated into the analysis using the principle of superposition, which holds that the combined response from multiple pumping wells is equal to the sum of the individual responses imparted by each pumping well (Todd 1980). Each P&T stress well was set to the flow rate observed during the 24 hours leading up to the shutdown. Table 4.5 contains the flow rates used in the analyses for the three shutdown events. In general, flow rates in the P&T wells prior to the shutdowns were very stable since they were being controlled by the HX P&T facility's SCADA system. One exception is well 199-H3-29 prior to the July 2019 shutdown, which was running at a stable flow rate until it experienced a brief stoppage and return to flow the day prior to the extended shutdown event.

4.2.4 October 2019 Shutdown Event

Prior to the initiation of the constant-rate pumping test in well 199-H3-22 in October 2019, all six RUM aquifer P&T extraction wells operating in the 100-H Area were shut down (Table 4.1). All RUM P&T wells were shut down in the test area for a period of nearly 4 days (94 hours) to create controlled

hydrologic conditions for the constant-rate test. Most of the wells in the test area were already configured with pressure sensors for monitoring and recording the constant-rate test, and this provided an ideal opportunity to evaluate the uppermost RUM aquifer's response to an area-wide and multi-well P&T shutdown event. Table 4.5 contains the pre-shutdown flow rates used in the analysis.

Table 4.5. Flow Rates for P&T Shutdown Event Stress Wells

Shutdown Event	Well Name	P&T ID[a]	Flow Rate[b] [L/min (gpm)]
June 2019	199-H3-2C	HE09	83 (22)
	199-H4-12C	HE10	163 (43)
	199-H3-28	HE12	170 (45)
	199-H3-29	HE14	57 (15)
July 2019	199-H3-28	HE12	170 (45)[c]
	199-H3-29	HE14	45 (12)[d]
October 2019	199-H3-2C	HE09	76 (20)
	199-H4-12C	HE10	110 (29)
	199-H3-22	HE11	125 (33)
	199-H3-28	HE12	170 (45)
	199-H3-9	HE13	38 (10)
	199-H3-29	HE14	49 (13)

(a) Unique identifier used by the 100-HX P&T facility for extraction wells from DOE/RL-2019-67.
(b) P&T flow data for HX wells were electronically transmitted through email correspondence from the P&T operations organization to PNNL in two separate batches, one sent on 1/1/2020 and another on 2/12/20. The flow rate value used in the analysis corresponds to the observed value during approximately 1 day prior to the shutdown event (unless otherwise noted).
(c) There were no P&T flow rate data available for 199-H3-28 in the 8 days leading up to the July shutdown event for an unknown reason. However, water-level data in this well indicate it was running at a near-constant rate during this time period prior to the shutdown event. The last available flow measurement prior to the shutdown test was used.
(d) Flows in well 199-H3-29 varied prior to the shutdown. The well was running consistently at about 49 L/min (13 gpm) until the day before the shutdown, when it stopped briefly and restarted, then increased to about 45 L/min (12 gpm) until the shutdown. A value of 45 L/min (12 gpm) was assumed for the for the analysis.

4.2.1 June 2019 Shutdown Event

The June 2019 shutdown event consisted of turning off the four 100-H RUM extraction wells that were active at the time: 199-H3-2C, 199-H3-28, 199-H3-29, and 199-H4-12C. Extraction well 199-H3-22 had not been connected to the HX P&T system yet, and extraction well 199-H3-9 was already down for maintenance prior to the June shutdown event. This shutdown event provided another area-wide stress, but with a slightly different stress-well configuration compared to the October 2019 shutdown event. Pre-shutdown flow rates are listed in Table 4.5.

4.2.2 July 2019 Shutdown Event

The July 2019 shutdown event involved turning off two of four P&T extraction wells running at the time. The stress wells were 199-H3-28 and 199-H3-29. Like the June 2019 event, wells 199-H3-22 and 199-H3-9 were not operating prior to the shutdown. The July event provides yet another variation since it involved fewer and more centrally located stress wells, as opposed to an area or system-wide shutdown event. Pre-shutdown flow rates are listed in Table 4.5.

4.2.3 Aquifer Properties Estimated from Shutdown Events

Table 4.6 lists the range of estimated aquifer hydraulic properties for the uppermost RUM aquifer and confining layer based on the analysis of the June, July, and October 2019 P&T shutdown events. Appendix A contains log-log plots of the observed shutdown responses and estimated aquifer properties from the type-curve matching analysis for each observation well location and shutdown event.

The results are organized into inner and outer regions of the test area, similar to the presentation of the constant-rate pumping test results. The assignment to the inner vs. outer region of the test area for the P&T shutdown tests is based the distance of the observation well from the nearest stress well involved in the shutdown event. There are some differences between results of the shutdown and constant-rate pumping test analyses that are related to the number and location of stress wells involved, but overall, the results are consistent with the P&T shutdown events.

For the June 2019 shutdown event where all four of the actively-pumping RUM aquifer extraction wells were shut off (Table 4.5), the T estimates from the inner region well responses show a very close agreement with each other and with the responses from the constant-rate pumping test (Table 4.6). In comparison, the T estimates from responses observed in the outer area wells 199-H3-32 and 199-H4-90 are a factor of 3 to 4 higher than those in the inner area (Table 4.6), but are very similar to the corresponding outer area estimates from the constant-rate analyses (Table 4.4).

Only two of the four active RUM extraction wells were shut off in the July 2019 event, and similar to the other shutdown events, the outer area observation wells exhibited the highest T and K' estimates (Table 4.6). The T estimate from the July shutdown response in well 199-H3-10 is 149.3 m^2/day, which is noticeably higher than estimates based on responses during the other two shutdown events (Table 4.6). However, this T estimate agrees more closely with the estimate of 118.5 m^2/day obtained from the constant-rate pumping test response (Table 4.4). The commonality between these two aquifer tests is the lack of a stress well nearby, which increases the radius or scale of investigation. This is another indication that the uppermost RUM aquifer exhibits spatial variability in hydraulic and/or physical properties, which become more evident as the radial distance between the observation well and stress wells increases.

The system-wide P&T shutdown event in October 2019 involved all six RUM extraction wells (Table 4.5). T estimates from the October shutdown event responses in the two outer region wells, 199-H3-32 and 199-H4-90, are consistent with those from the other two shutdown events (Table 4.6) and the constant-rate pumping test (Table 4.4). The T estimates from the October 2019 shutdown response are slightly higher for observation wells 199-H3-12 and 199-H3-13 compared to the other three aquifer tests (Table 4.4 and Table 4.6); whereas the T estimate from the October 2019 shutdown response in well 199-H3-10 is considerably lower than the June 2019 shutdown event and the constant-rate pumping test.

Storativity (S) estimates based on the RUM P&T shutdown responses for all observations (inner and outer regions combined) range from 1.8×10^{-4} to 9.0×10^{-4}, with the highest values coming from responses analyzed in the outer area wells 199-H3-32 and 199-H4-90 (Table 4.6), which were consistently located farther from the P&T stress wells during the shutdown events.

Table 4.6. Uppermost RUM Aquifer and Confining Layer Hydraulic Property Estimates from P&T Shutdown Events in 2019

Shutdown Event	Region of the Test Area	Observation Well	T (m^2/day)	K (m/day)	S	K' (m/day)
June 2019	Inner	199-H3-10	43.0	4.4	3.2E-04	1.4E-02
		199-H3-12	46.1	4.7	2.8E-04	2.0E-02
		199-H3-13	47.1	4.8	2.3E-04	1.4E-02
		199-H3-22	45.2	4.6	2.5E-04	1.7E-02
		Geometric Mean	**45.3**	**4.6**	**2.7E-04**	**1.6E-02**
	Outer	199-H3-32	153.7	15.7	5.6E-04	4.9E-02
		199-H4-90	173.5	17.7	8.5E-04	4.5E-02
		Geometric Mean	**163.3**	**16.7**	**6.9E-04**	**4.7E-02**
July 2019	Inner	199-H3-12	47.4	4.8	2.7E-04	2.1E-02
		199-H3-13	27.7	2.8	1.9E-04	2.1E-02
		199-H3-22	34.6	3.5	2.0E-04	2.2E-02
		Geometric Mean	**35.7**	**3.6**	**2.2E-04**	**2.1E-02**
	Outer	199-H3-10	149.3	15.2	1.4E-04	3.4E-03
		199-H3-32	173.7	17.7	6.4E-04	3.9E-02
		Geometric Mean	**161.0**	**16.4**	**3.0E-04**	**1.1E-02**
October 2019	Inner	199-H3-10	67.4	6.9	2.5E-04	1.2E-02
		199-H3-12	77.2	7.9	1.6E-04	4.2E-03
		199-H3-13	63.4	6.5	1.4E-04	2.7E-03
		Geometric Mean	**69.1**	**7.0**	**1.8E-04**	**5.1E-03**
	Outer	199-H3-32	172.1	17.6	7.4E-04	3.1E-02
		199-H4-90	214.4	21.9	1.1E-03	3.0E-02
		Geometric Mean	**192.1**	**19.6**	**9.0E-04**	**3.1E-02**
P&T Shutdown Test Estimates Combined (n=16)		**Min**	**27.7**	**2.8**	**1.4E-04**	**2.7E-03**
		Max	**214.4**	**21.9**	**1.1E-03**	**4.9E-02**
		Geometric Mean	**77.3**	**7.9**	**3.2E-04**	**1.6E-02**

T = transmissivity of the RUM aquifer (T = K/b)
K = hydraulic conductivity of the RUM aquifer calculated using b = 9.8 m (Table 2.2)
S = storativity of the RUM aquifer
b = thickness of the RUM aquifer
K' = vertical hydraulic conductivity of the RUM aquitard (confining layer)

5.0 Discussion

There has been uncertainty regarding the lateral continuity and hydraulic character of the water-bearing units in the RUM and how this impacts remedial optimization of Cr(VI) contamination in the uppermost RUM aquifer in the 100-HR-3 OU. The hydrologic evaluation in this report presents a suite of complimentary aquifer pumping test analyses and results within the 100-H test area. The results presented in Section 4.0 identify lateral hydraulic continuity in the uppermost RUM aquifer at spatial scales larger than previously recognized and provide a range of hydraulic properties for the RUM aquifer within the 100-H Area.

This section provides an integrated discussion of results and impacts from this evaluation, organized into three discussion categories relating back to the areas of uncertainty and research needs identified in Section 3.0. These include 1) lateral hydraulic continuity of the RUM aquifer, 2) RUM aquifer hydraulic and storage properties within the 100-H Area [including the high-concentration portion of the Cr(VI) plume], and 3) the demonstration and application of P&T shutdown tests for aquifer hydraulic characterization.

5.1 Lateral Hydraulic Continuity of the Uppermost RUM Aquifer

The presence of the RUM confining layer and uppermost aquifer has been identified in a growing number of borehole locations throughout the 100-H Area based on lithologic and geophysical interpretations (CP-65222). This borehole geologic information is being used by the site contractor to develop a site-specific geologic framework model for intra-RUM units (CP-65222). The additional aquifer hydrologic characterization information provided in this evaluation supports previous studies (Section 2.3) indicating there is lateral hydraulic connectivity between RUM aquifer wells in the 100-H Area. Responses from the constant-rate pumping test in well 199-H3-22, performed in October 2019, indicate there is hydraulic connectivity extending laterally across the test area more than 500 m (Figure 5.1). Distinguishing the RUM as a laterally connected aquifer conceptually and hydraulically within the 100-H Area is significant to the CSM and impacts modeling efforts supporting optimization of the P&T system.

Examining the larger, kilometer-scale lateral continuity of the RUM aquifer outside of the 100-H Area was outside the scope of this evaluation. As additional boreholes or wells are drilled and constructed in the region between the Horn and the 100-H Area in the future, this uncertainty could be investigated using similar hydrologic methods as demonstrated in this evaluation (e.g., constant-rate pumping or P&T shutdown events).

5.2 RUM Aquifer Properties

Natural aquifer systems are inherently heterogenous, despite being commonly represented otherwise in analytical models. The hydrologic evaluation presented here relied on type-curve matching of observed responses in many different observation wells distributed throughout the 100-H test area (Figure 4.1). Type-curve matches were based on the leaky-confined aquifer model of Hantush and Jacob (1955), which assumes no confining layer storage.

The responses in observation wells to aquifer pumping tests are determined by the bulk or volume-weighted aquifer properties within the radius of investigation (Butler and Liu 1993; Oliver 1993; Meier et al. 1998). Estimates associated with analyses of responses exhibited in individual observation wells are presented in this hydrologic evaluation (Table 4.4 and Table 4.6). However, it is important to emphasize that they represent the larger-scale bulk properties of the RUM aquifer within the test area. Geometric

mean values were calculated for the inner and outer regions of the test area (Table 4.4), and these are considered more appropriate and spatially-representative estimates describing the range of estimated hydraulic properties for the RUM aquifer within the 100-H test area.

Similarities and differences between the results from the constant-rate pumping test in well 199-H3-22 provide insight into the hydrologic character of the uppermost RUM aquifer in the 100-H Area. First, the results suggest that the aquifer is relatively uniform in hydraulic and storage properties within the inner region of the test area based on the narrow range of estimates obtained from the five inner area wells (Table 4.4). However, estimates from responses in the five wells in the outer region of the test area indicate that more variability and the geometric means of the estimates are markedly higher compared to the inner area (Table 5.1 and Figure 5.1). This observed increase in T, S, and K' away from the inner region of the test indicates the presence of lateral heterogeneity in the aquifer. The higher values of all three aquifer properties suggest there may be an increase in effective aquifer thickness or higher leakage through the RUM confining layer within the radius of investigation. Dependency of aquifer properties, such as K, on the scale of investigation has been previously noted by others (Hunt 2006; Fallico et al. 2010).

Table 5.2 contains the range and geometric mean calculated for the entire collection of T, K, S, and K' estimates for the uppermost RUM aquifer based on the analyses of a constant-rate pumping test in 199-H3-22 and three different P&T shutdown events. A total of 36 aquifer pumping test responses were analyzed from 10 different observation well locations throughout the 100-H Area. Comparisons with the results from this study, listed in Table 5.2, and those previously reported for RUM wells in the 100-H Area (Table 2.3) indicate good agreement (Table 4.4).

Table 5.1. Geometric Means of Aquifer Hydraulic Property Estimates for the Uppermost RUM Aquifer in the Inner and Outer Test Area Regions of the Constant-Rate Pumping Test in Well 199-H3-22 (see Figure 4.1)

	Inner Region	Outer Region
Transmissivity (T)	49.9 m^2/day	157.6 m^2/day
Hydraulic conductivity[(a)] (K)	5.1 m/day	17.0 m/day
Storativity (S)	2.0x10-4	7.3x10-4
Confining layer vertical hydraulic conductivity (K')	$5.1x10^{-3}$ m/day	$2.5x10^{-2}$ m/day

(a) K = T/b; where b = average aquifer thickness (Table 2.2)

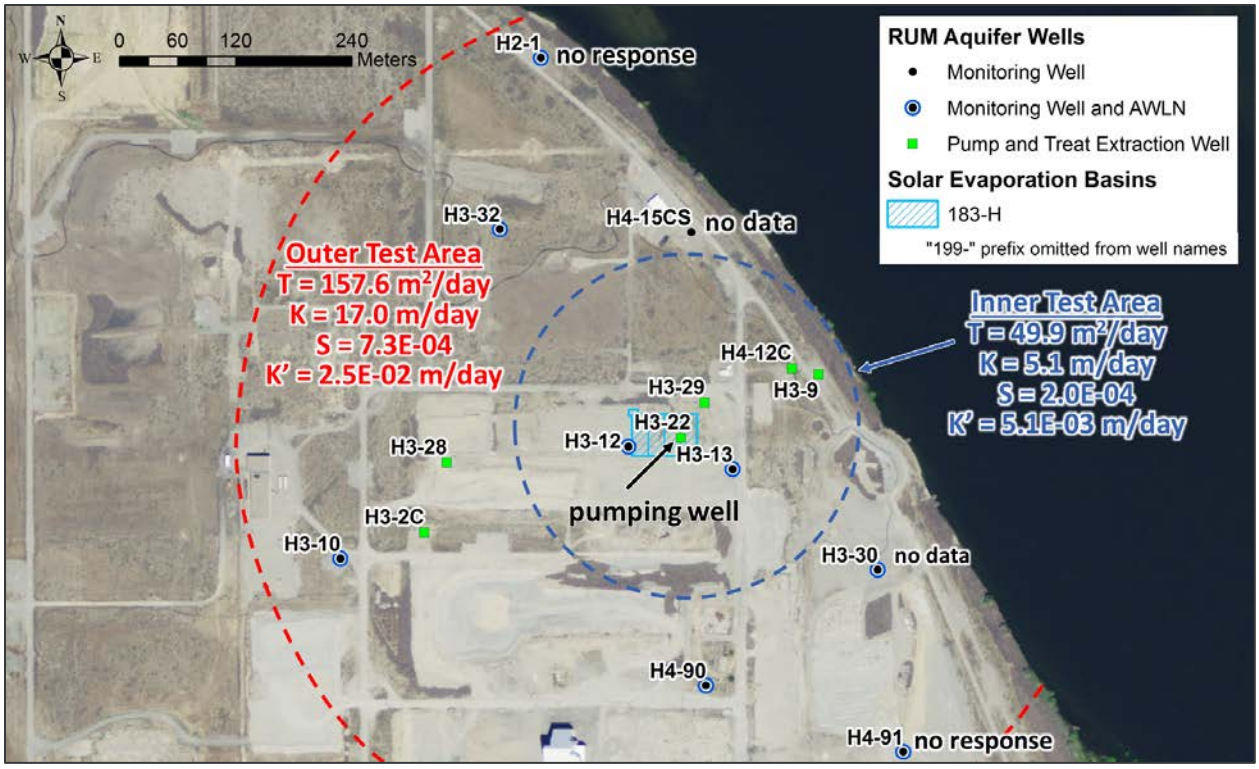

Figure 5.1. Map showing the geometric mean of estimated aquifer transmissivity (T), storativity (S), hydraulic conductivity (K), and confining layer vertical hydraulic conductivity (K') for the uppermost RUM aquifer within inner and outer regions of the 100-H test areas. Results are based on the constant-rate pumping test performed in well 199-H3-22 in October 2019.

Table 5.2. Range and Geometric Means of Aquifer Hydraulic Property Estimates for the Uppermost RUM in the 100-H Area from Multiple Aquifer Tests Performed in 2019

	Minimum[(a)]	Maximum	Geometric Mean
Transmissivity (T)	27.7m^2/day	236.8 m^2/day	83.3m^2/day
Hydraulic conductivity[(b)] (K)	2.8 m/day	24.2 m/day	8.5 m/day
Storativity (S)	$1.4x10^{-4}$	$1.3x10^{-3}$	$3.4x10^{-4}$
Confining layer vertical hydraulic conductivity (K')	$2.7x10^{-3}$ m/day	$4.9x10^{-2}$ m/day	$1.3x10^{-2}$ m/day

(a) Minimum, maximum, and geometric means were calculated using all estimates from the constant-rate pumping test in well 199-H3-22 and the three P&T shutdown events (n=36).
(b) K = T/b; where b = average aquifer thickness (Table 2.2).

5.3 Demonstration and Application of P&T Shutdown Events for Aquifer Characterization

There is an increasing need to perform aquifer characterization activities in test areas with an active P&T remedy. An approach for analyzing P&T shutdown responses was demonstrated using hydraulic responses from three shutdown events occurring in 2019, and results were compared to those from a constant-rate pumping test in the same wells. The shutdown events varied in the number and locations of P&T wells being turned off (referred to as stress wells).

The aquifer hydraulic properties for the RUM aquifer estimated from analysis of the June, July, and October 2019 shutdown events (Table 4.6) were generally very consistent with those obtained from the constant-rate pumping test (Table 4.4). Despite the fact that each of the three shutdowns involved a different number and locations of stress wells, similar estimates for the inner and outer regions of the test area were obtained (Table 4.6). The consistency and similarity of the results from the P&T shutdown events is encouraging for future applications of aquifer characterization in settings where there is an active P&T operating.

6.0 Conclusions

A hydrologic evaluation of the RUM aquifer in the Hanford Site 100-H Area was performed to help address areas of uncertainty regarding the lateral continuity of the RUM aquifer and characterize aquifer properties within the high-concentration portion of the RUM Cr(VI) plume. The evaluation consisted of both constant-rate pumping tests and P&T shutdown events. The evaluation demonstrated the utility of P&T shutdown events for aquifer characterization.

Hydraulic responses from the aquifer pumping tests performed in this evaluation provide a definitive indication that the uppermost RUM aquifer is a semiconfined or leaky-confined aquifer. This is consistent with previous investigations (SGW-60571). Results confirm that the aquifer is laterally connected at distances spanning 500 meters or more within the 100-H test area, a lateral distance larger than previously recognized. The results from a constant-rate pumping test in the P&T extraction well 199-H3-22 indicate 1) the aquifer hydraulic properties are uniform within an inner region of the 100-H Test area, 2) there is some level of spatial variability within the 100-H test area, and 3) aquifer properties estimated from responses in observation wells located in the outer region of the test area appear to be higher in transmissivity (T), storativity (S), and confining layer vertical hydraulic conductivity (K'). This suggests that as larger portions of the aquifer are investigated, the presence of heterogeneities and their associated impact on observation well response become more evident. It is speculated there are increases in the effective aquifer thickness and/or relatively higher rates of vertical leakage through the RUM confining layer to the unconfined aquifer at some unknown location(s) within the radius of investigation.

These results inform the conceptual site model (CSM) for the RUM aquifer and will impact future remediation of Cr(VI) in the follow ways: 1) Results strongly indicate the uppermost RUM aquifer is a laterally connected aquifer conceptually and hydraulically within the 100-H Area and should be represented as a continuous hydrologic layer in predictive fate and transport modeling, and 2) the aquifer hydraulic properties in the high-concentration portion of the Cr(VI) plume provided in this evaluation can be used as input parameters in model simulations to more accurately predict the effective radius of influence, number of extraction wells needed, and the remedial effect P&T extraction wells have on removal of mass or hydraulic control of Cr(VI) within the RUM aquifer. All of which directly impact the time to cleanup and cost for remediation of the RUM aquifer.

In addition to the constant-rate pumping test, the hydrologic evaluation included the analysis of three P&T shutdown events involving multiple RUM extraction wells that occurred in June, July, and October 2019. P&T shutdown events conceptually involve turning off one or more of P&T (stress) wells, while continuing to pump other P&T wells in the area at a constant rate. The recovery component of observed pressure responses to the shutdown events was analyzed similarly to a constant-rate pumping test. Results from all three P&T shutdown events tests were consistent with the results from the 2019 constant-rate pumping test. This evaluation demonstrates the applicability of P&T shutdown events to inform aquifer characterization that is less disruptive to P&T operations and offers potential cost savings over traditional constant-rate testing approaches. Opportunistic analysis of shutdown events that have or will occur for operational maintenance purposes is recommended as an additional hydrologic characterization tool. Planned and coordinated P&T shutdown events could also be designed with specific hydrologic test objectives in mind.

7.0 Quality Assurance

This work was performed in accordance with the PNNL Nuclear Quality Assurance Program (NQAP). The NQAP complies with the DOE Order 414.1D, *Quality Assurance*. The NQAP uses NQA-1-2012, *Quality Assurance Requirements for Nuclear Facility Application* as its consensus standard and NQA-1-2012 Subpart 4.2.1 as the basis for its graded approach to quality.

8.0 References

Agarwal RG. 1980. “A New Method to Account for Producing Time Effects when Drawdown Type Curves are Used to Analyze Pressure Buildup and Other Test Data.” *SPE Paper 9289 presented at the 55th SPE Annual Technical Conference and Exhibition*, Dallas, TX, Sept. 21-24, 1980.

Bourdet DJ, A Ayoub, and YM Pirard. 1989. “Use of pressure derivative in well-test interpretation.” *SPE Formation Evaluation* June 1989:293-302.

Butler JJ and W Liu. 1993. “Pumping Tests in Non-Uniform Aquifers: The Radially Asymmetric Case.” *Water Resources Research* 29(2):259-269

Cooper HH, Jr. and CE Jacob. 1946. “A generalized graphical method for evaluating formation constants and summarizing well-field history.” *American Geophysical Union, Transactions* 27(4):526-534.

CP-65222. (Pending). *Model Package Report: Site-Specific Geoframework Model of the 100-HR-3 Intra-RUM Semi-Confined Aquifer System*. Rev. 0, CH2M Hill Plateau Remediation Company, Richland, Washington.

DOE/RL-2010-95. 2014. *Remedial Investigation/Feasibility Study for the 100-DR-1, 100-DR-2, 100-HR-1, 100-HR-2, and 100-HR-3 Operable Units*. Rev. 0, U.S. Department of Energy, Richland Operations Office, Richland, Washington.

DOE/RL-2017-13. (Pending). *Remedial Design/Remedial Action Work Plan for the 100-DR-1, 100-DR-2, 100-HR-1, 100-HR-2, and 100-HR-3 Operable Units*. Draft A, U.S. Department of Energy, Richland Operations Office, Richland, Washington.

DOE/RL-2019-66. 2020. *Hanford Site Groundwater Monitoring Report for 2019*. Rev. 0, U.S. Department of Energy, Richland Operations Office, Richland, Washington.

DOE/RL-2019-67. 2020. *Calendar Year 2019 Annual Summary Report for the 100-HR-3 and 100-KR-4 Pump and Treat Operations, and 100-NR-2 Groundwater Remediation*. Rev. 0, U.S. Department of Energy, Richland Operations Office, Richland, Washington.

Duffield GM. 2007. *AQTESOLV for Windows User’s Guide*, Version 4.5. HydroSOLVE, Inc., Reston, Virginia. http://www.aqtesolv.com

Duffield GM. 2009. “Upgrading Aquifer Test Analysis, by William C. Walton.” *Ground Water Comment Discussion Paper* 47(6):756-757.

Fallico C, S De Bartolo, S Troisi and M Veltri. 2010. “Scaling Analysis of Hydraulic Conductivity and Porosity on a Sandy Medium of An Unconfined Aquifer Reproduced in the Laboratory.” *Geoderma* 160(2010):3-12.

Ferris JG, DB Knowles, RH Brown and RW Stallman. 1962. “Theory of Aquifer Tests.” *U.S. Geological Survey Water-Supply Paper* 1536-E.

Freeze RA and JA Cherry. 1979. *Groundwater*. Prentice-Hall, Englewood Cliffs, New Jersey.

Hantush MS and CE Jacob. 1955. “Non-steady Radial Flow in an Infinite Leaky Aquifer.” *Transactions of the American Geophysical Union* 36(1):95-100.

Hantush MS. 1962 “Aquifer Tests on Partially Penetrating Wells.” *Transactions of the American Society of Civil Engineers* 127(1):284-308.

Hunt AG. 2006. “Scale-Dependent Hydraulic Conductivity in Anisotropic Media from Dimensional Cross-Over.” *Hydrogeology Journal* 14:499-507.

Hyder Z, JJ Butler, CD McElwee and L Wenzhi. 1994. “Slug tests in partially penetrating wells.” *Water Resources Research* 30(11):2945-2957.

Lohman SW. 1972. “Ground-Water Hydraulics.” *U.S. Geological Professional Paper 708*.

Mackley RD, ML Rockhold, R Ekre, and I Demirkanli. 2020. *Aquifer Hydraulic Testing and Characterization Plan for the Ringold Formation Unit A in the Hanford 200-ZP-1 Groundwater Operable Unit and Vicinity*. PNNL-30163, Pacific Northwest Laboratory, Richland, Washington.

Meier PM, J Carrera, and X Sanchez-Vila. 1998. “An Evaluation of Jacob's Method for the Interpretation of Pumping Tests in Heterogeneous Formations.” *Water Resources Research* 34(5):1011– 1025.

Oliver DS. 1993. “The Influence of Nonuniform Transmissivity and Storativity on Drawdown.” *Water Resources Research* 29(1):169-178.

PNL-6468. 1987. *Ground-Water Monitoring Compliance Projects for Hanford Site Facilities, Progress Report for the Period April 1 to June 30, 1987*. Rev. 0, Pacific Northwest Laboratory, Richland, Washington.

Rasmussen TC and LA Crawford. 1997. “Identifying and removing barometric pressure effects in confined and unconfined aquifers.” *Ground Water* 35(3):502-511.

SGW-47776. 2010. *Aquifer Testing and Rebound Study in Support of the 100-H Deep Chromium Investigation*. Rev. 0, CH2M HILL Plateau Remediation Company, Richland, Washington.

SGW-60571. 2017. *Aquifer Testing of the First Water-Bearing Unit in the RUM at 100-H*. Rev. 0, CH2M Hill Plateau Remediation Company, Richland, Washington.

Spane FA, Jr. 1993. *Selected Hydraulic Test Analysis Techniques for Constant-Rate Discharge Tests*. PNL-8539, Pacific Northwest Laboratory, Richland, Washington.

Spane FA. 2010. *Large-Scale Pumping Test Recommendations for the 200-ZP-1 Operable Unit*. PNNL-19695, Pacific Northwest National Laboratory, Richland, Washington.

Theis CV. 1935. “The relation between the lowering of the piezometric surface and the rate and duration of discharge of a well using groundwater storage.” *Transactions of the American Geophysical Union* 16:519-524.

Todd DK. 1980. *Groundwater Hydrology*. John Wiley & Sons, New York, 535p..

Appendix A – Additional Hydrologic Evaluation Figures

A.1 Additional Constant-Rate Pumping Test Analysis Figures

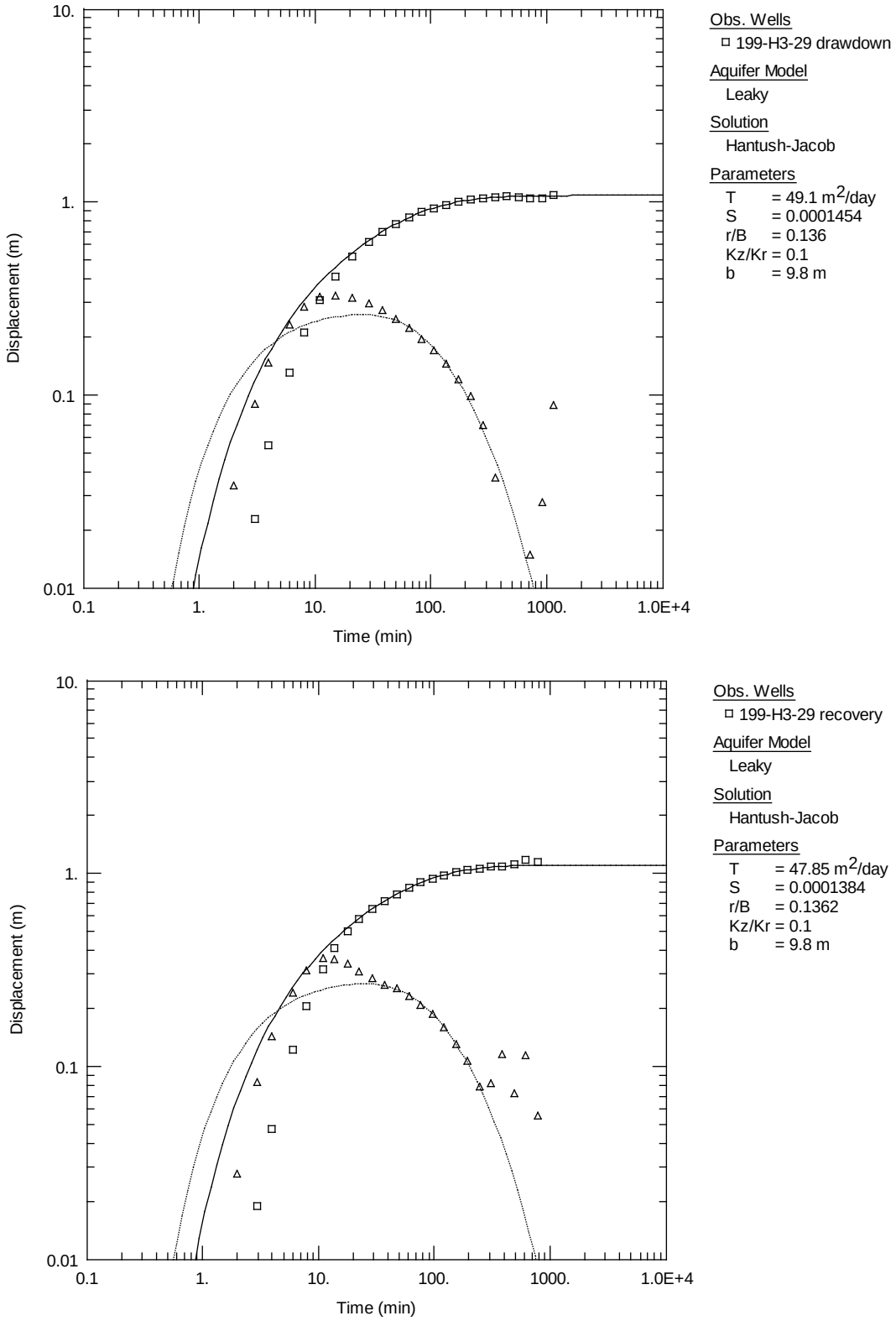

Figure A.1. Type-curve matches to the drawdown (upper plot) and recovery (lower plot) and derivative responses observed in well 199-H3-29 to the constant-rate pumping test in well 199-H3-22.

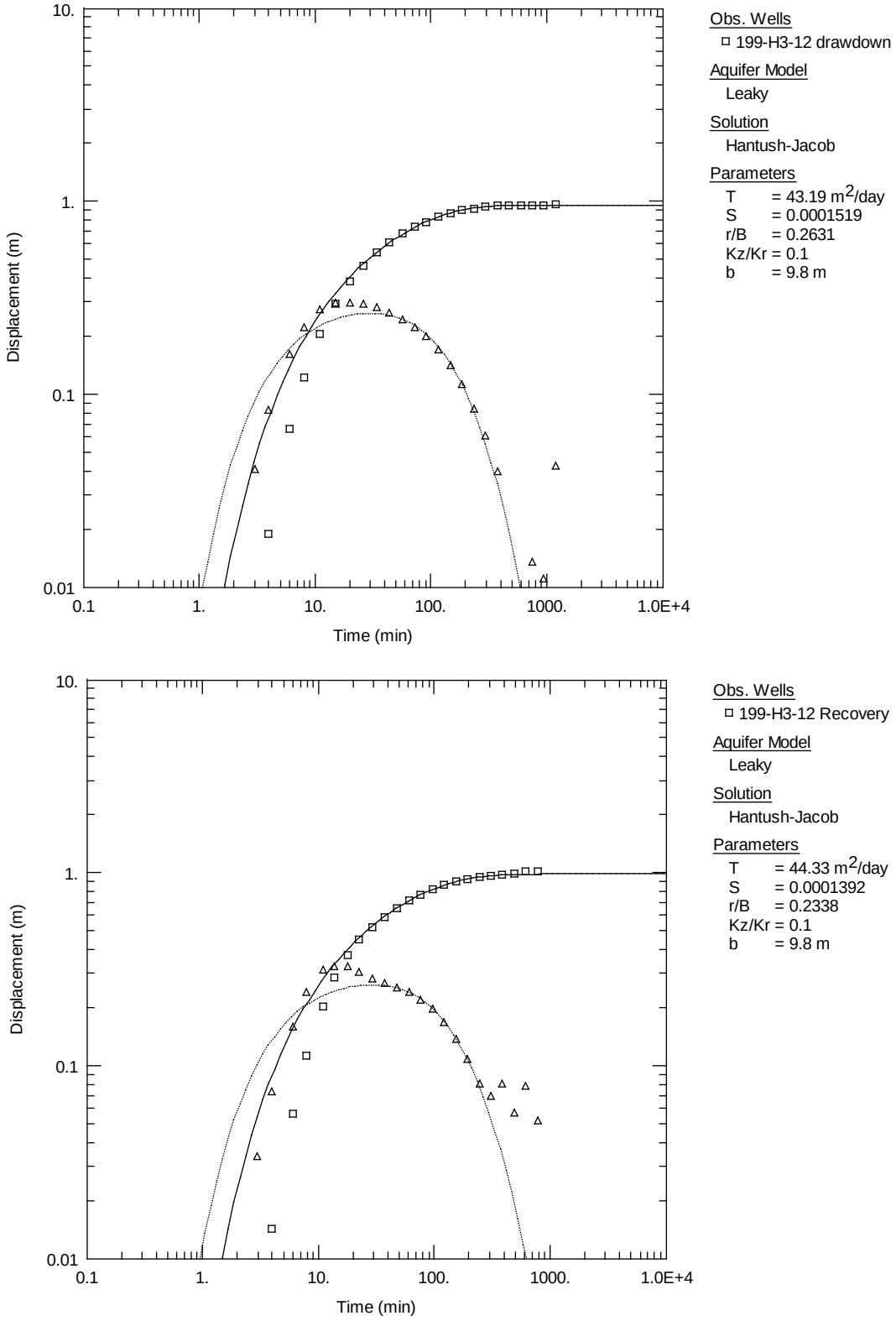

Figure A.2. Type-curve matches to the drawdown (upper plot) and recovery (lower plot) and derivative responses observed in well 199-H3-12 to the constant-rate pumping test in well 199-H3-22.

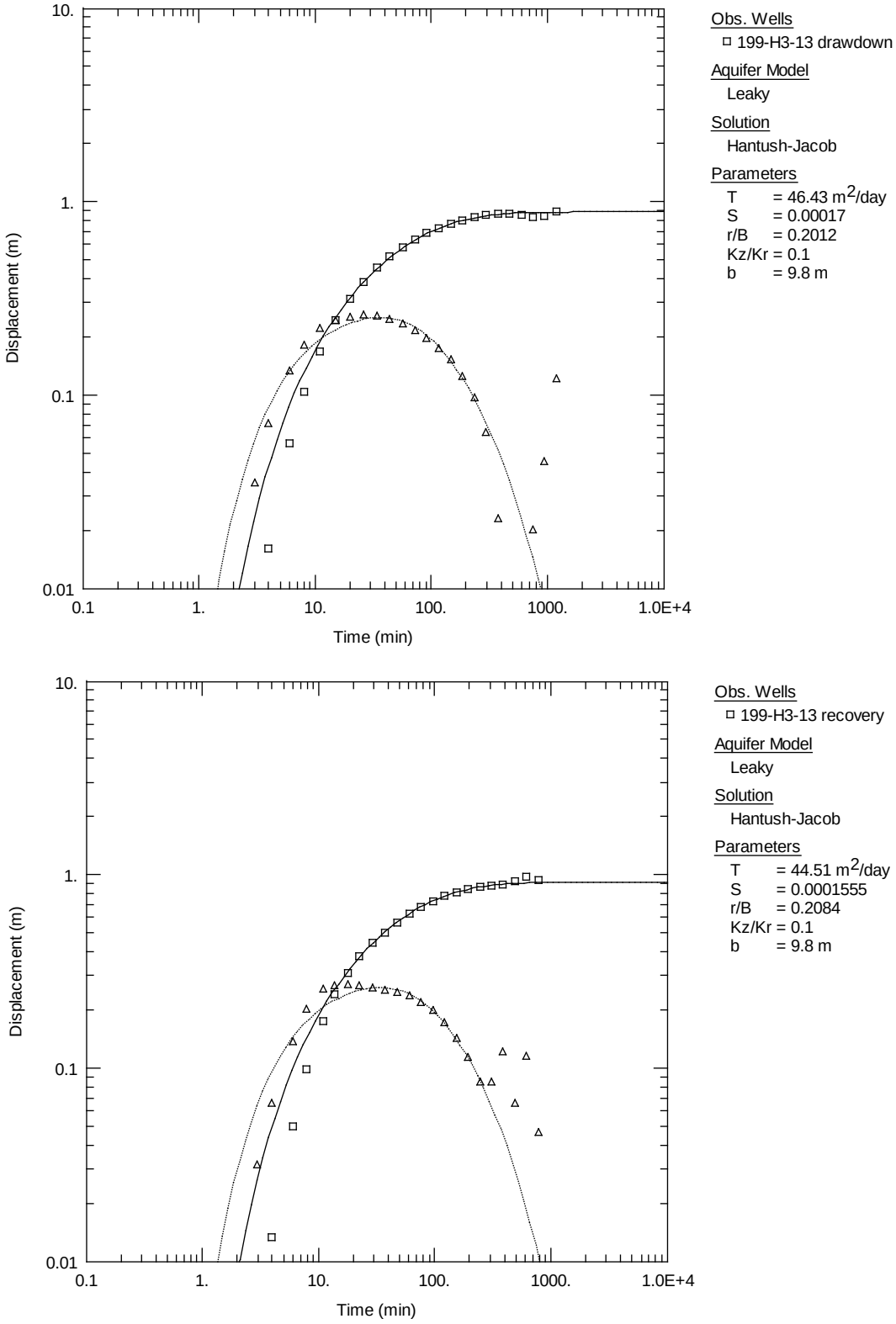

Figure A.3. Type-curve matches to the drawdown (upper plot) and recovery (lower plot) and derivative responses observed in well 199-H3-13 to the constant-rate pumping test in well 199-H3-22.

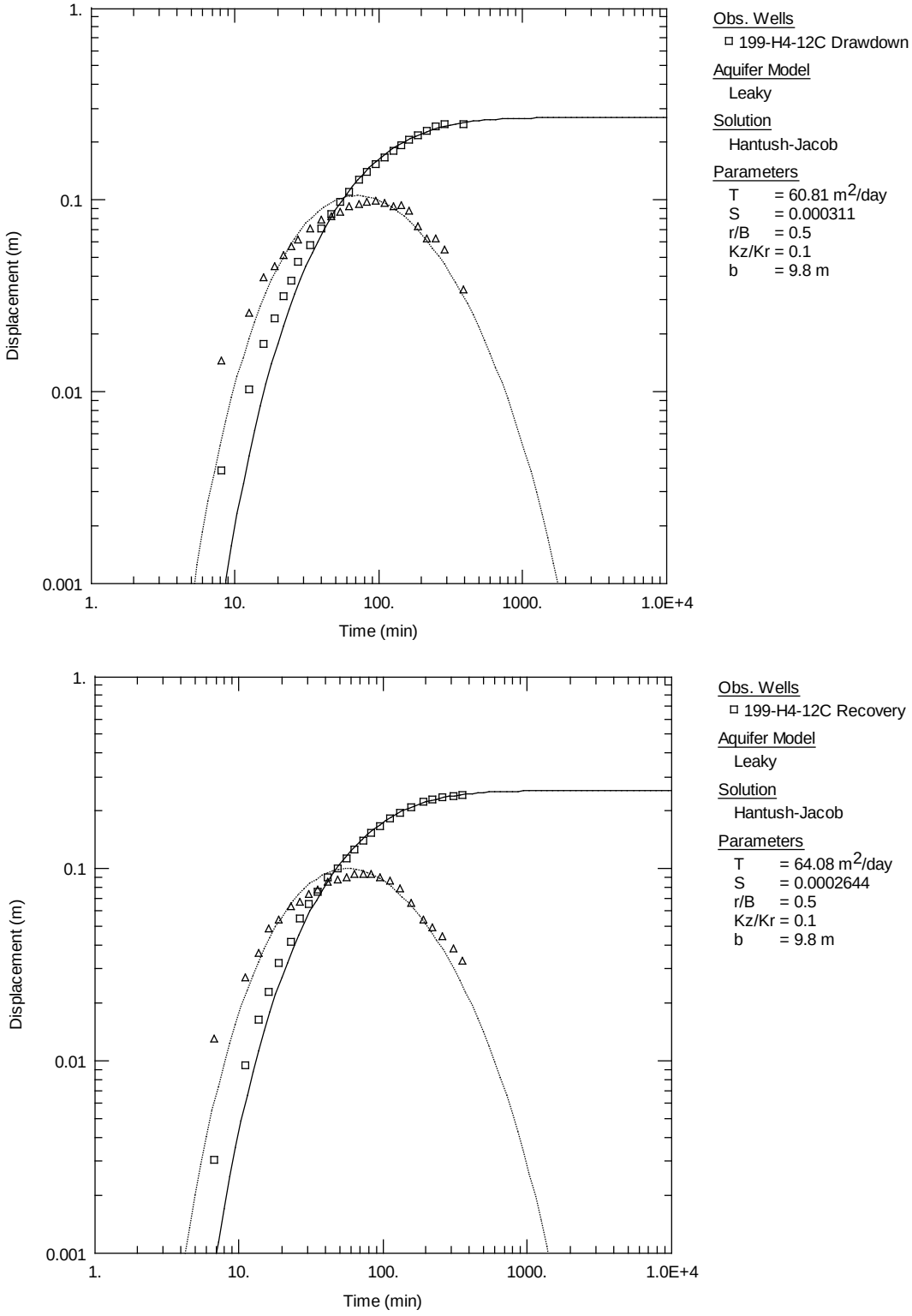

Figure A.4. Type-curve matches to the drawdown (upper plot) and recovery (lower plot) and derivative responses observed in well 199-H4-12C to the constant-rate pumping test in well 199-H3-22.

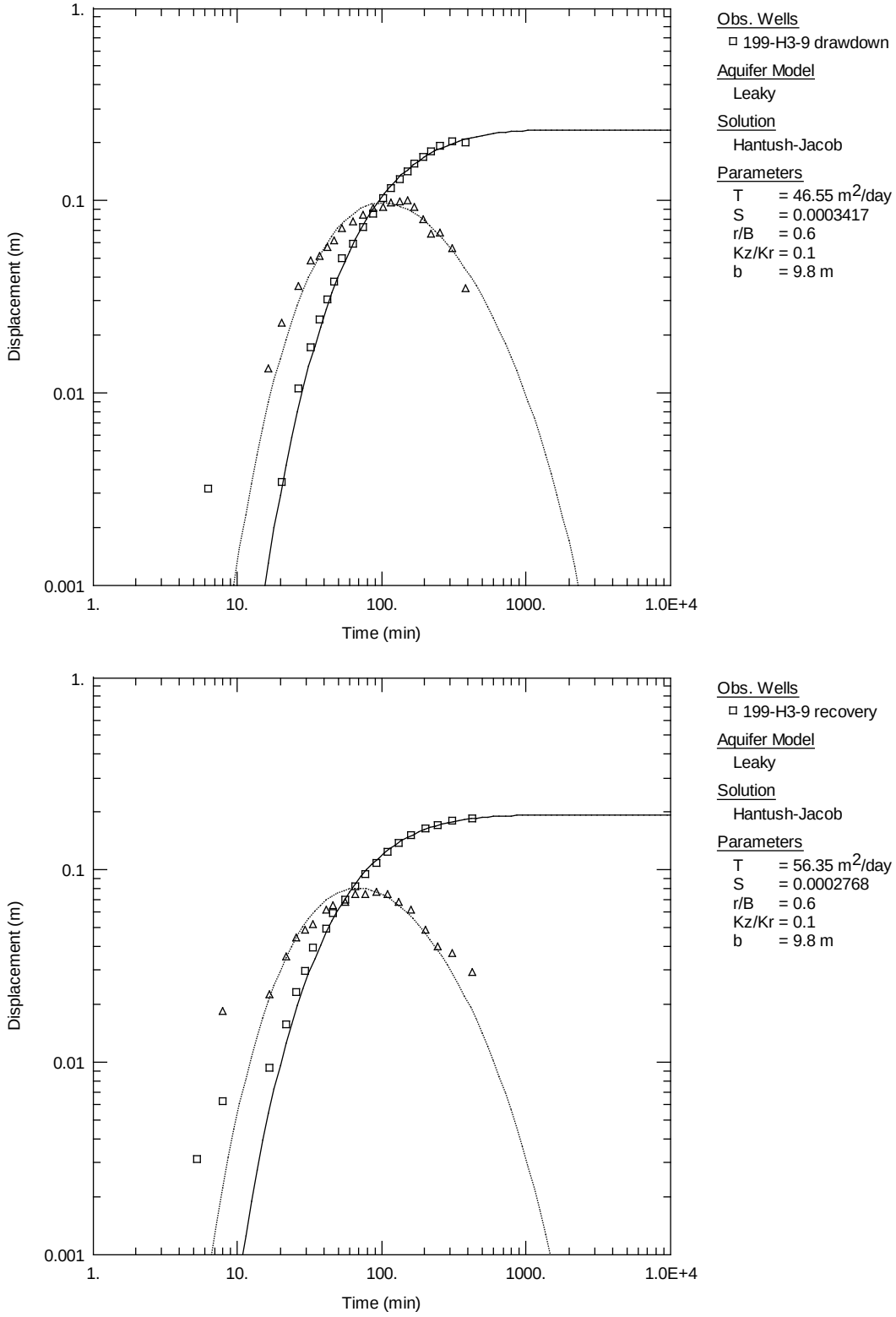

Figure A.5. Type-curve matches to the drawdown (upper plot) and recovery (lower plot) and derivative responses observed in well 199-H3-9 to the constant-rate pumping test in well 199-H3-22.

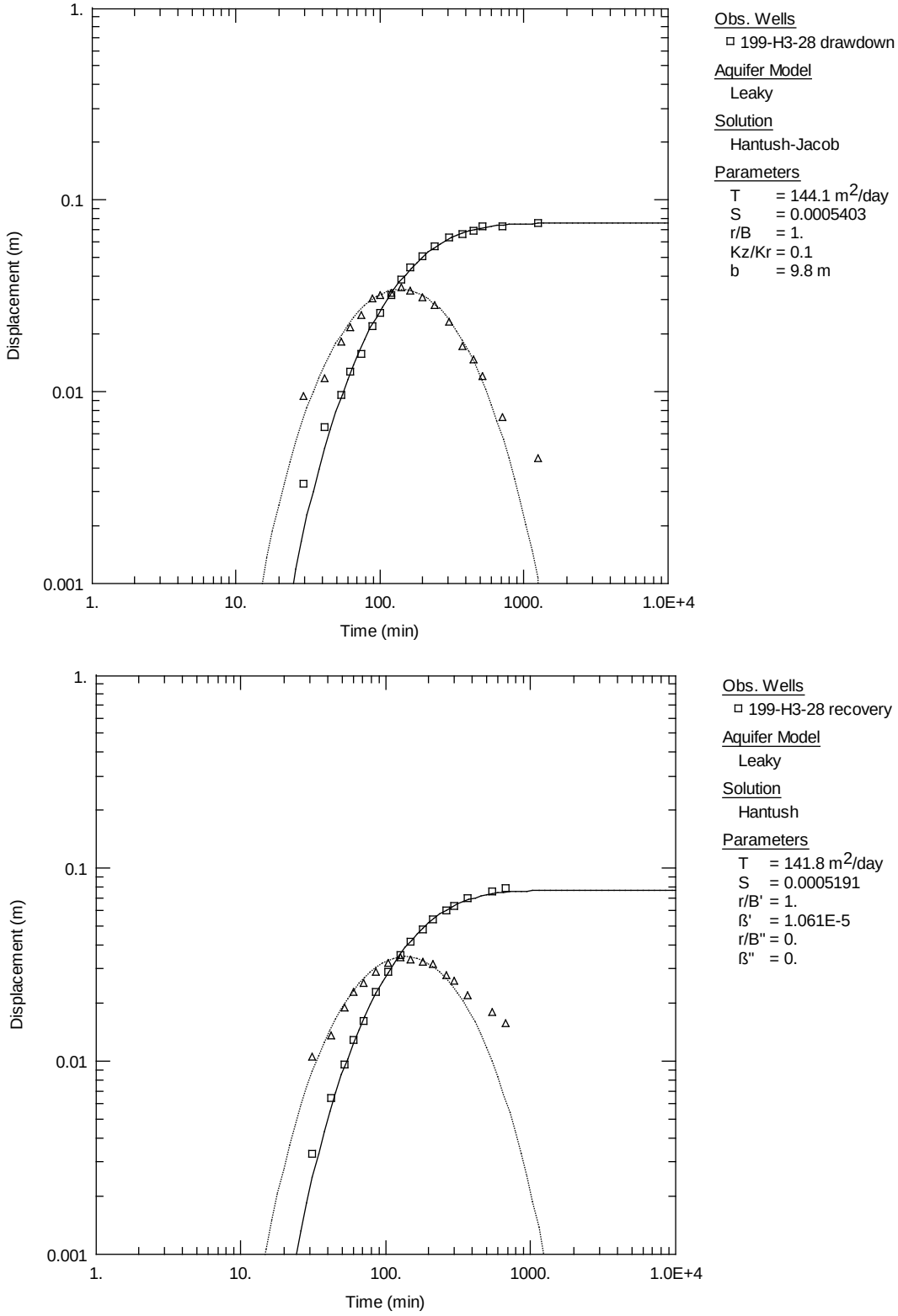

Figure A.6. Type-curve matches to the drawdown (upper plot) and recovery (lower plot) and derivative responses observed in well 199-H3-28 to the constant-rate pumping test in well 199-H3-22.

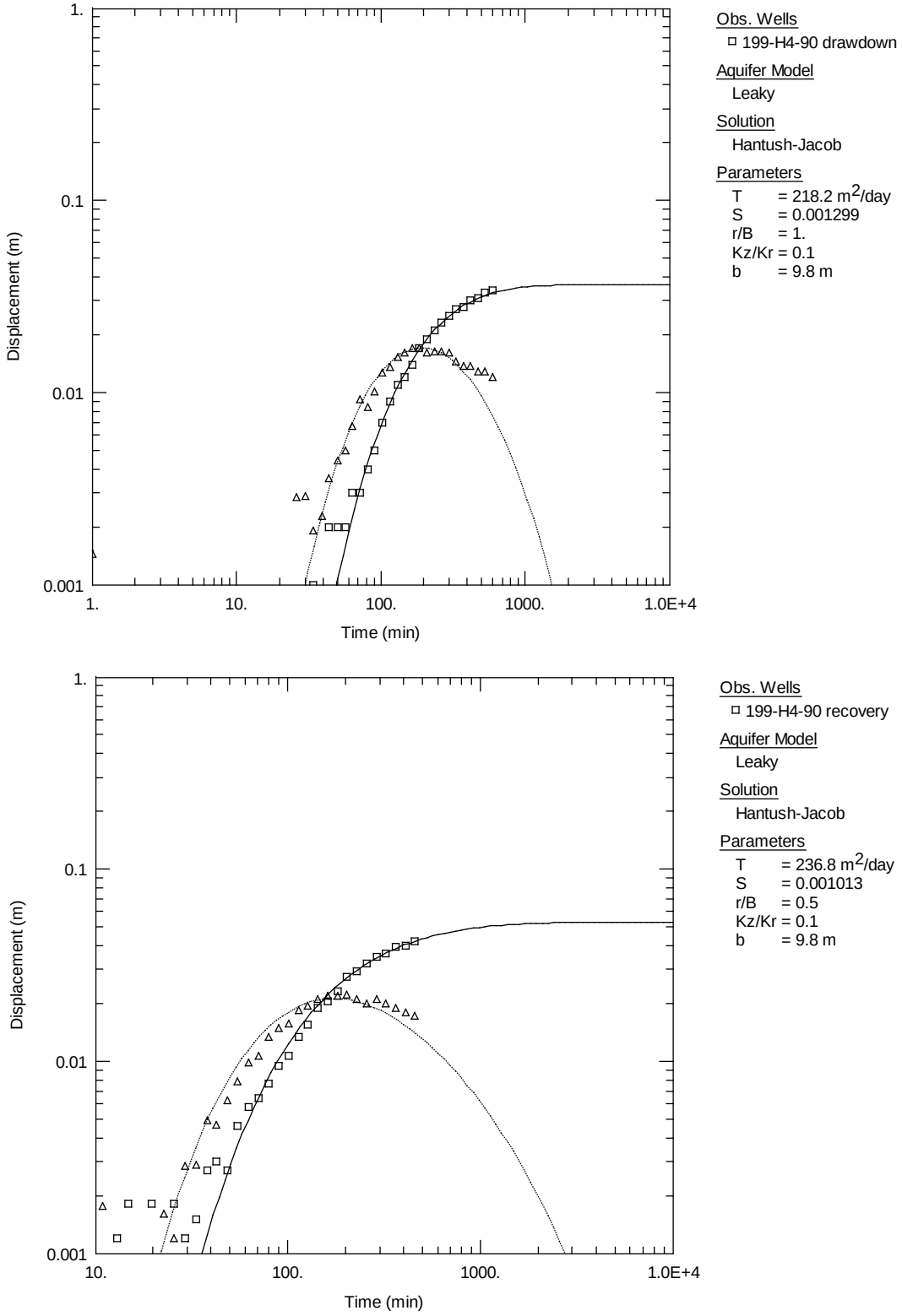

Figure A.7. Type-curve matches to the drawdown (upper plot) and recovery (lower plot) and derivative responses observed in well 199-H4-90 to the constant-rate pumping test in well 199-H3-22.

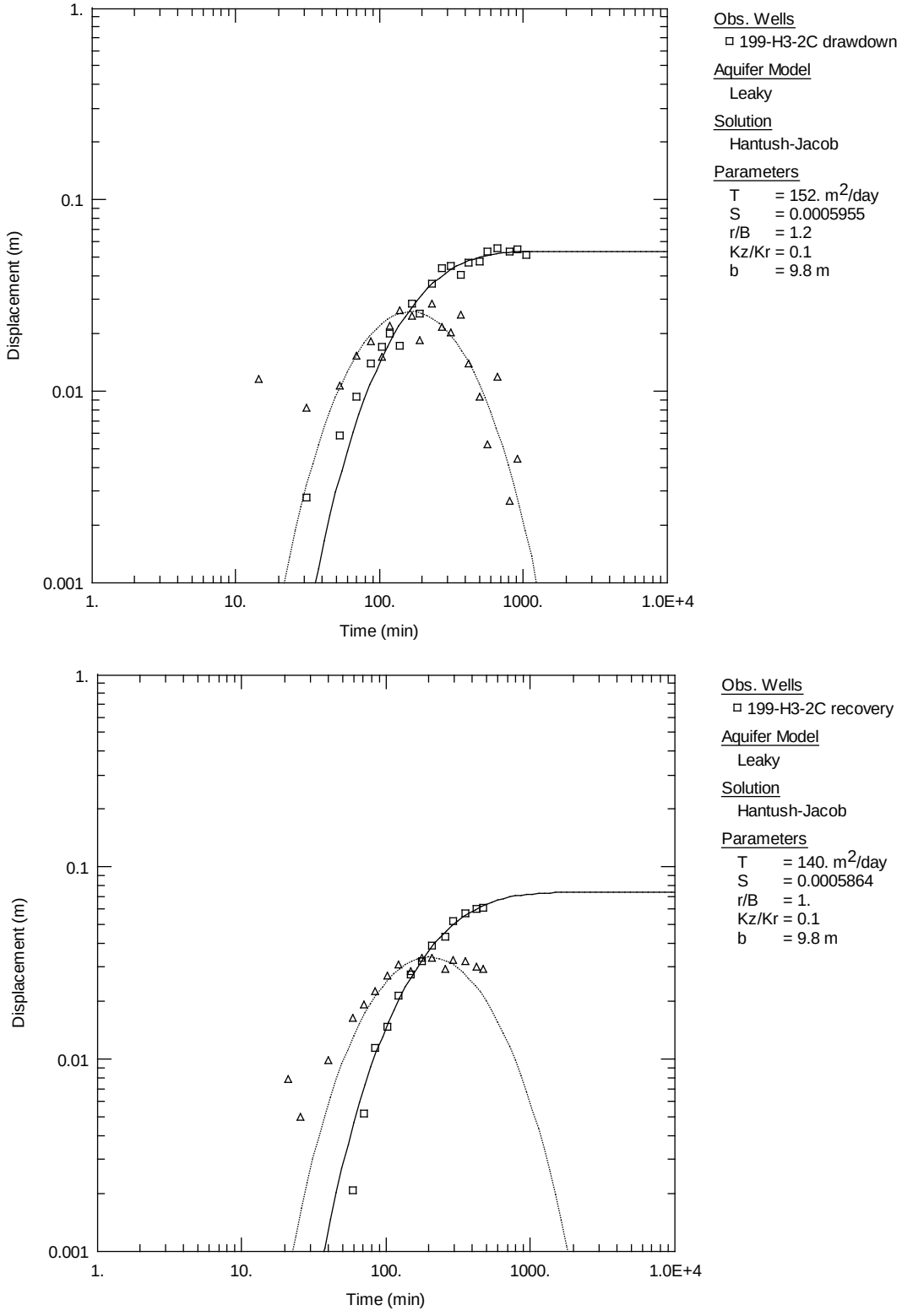

Figure A.8. Type-curve matches to the drawdown (upper plot) and recovery (lower plot) and derivative responses observed in well 199-H3-2C to the constant-rate pumping test in well 199-H3-22.

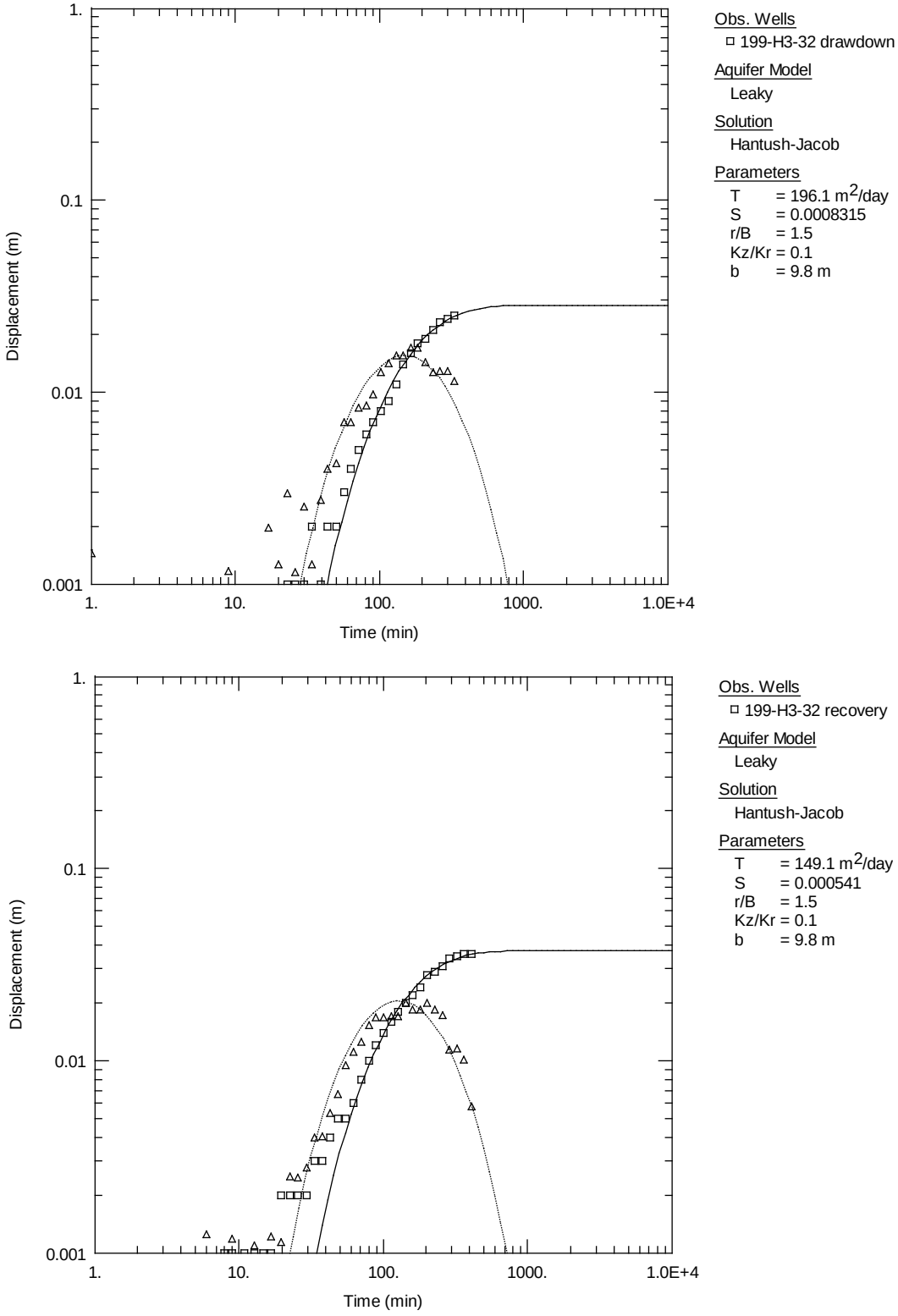

Figure A.9. Type-curve matches to the drawdown (upper plot) and recovery (lower plot) and derivative responses observed in well 199-H3-32 to the constant-rate pumping test in well 199-H3-22.

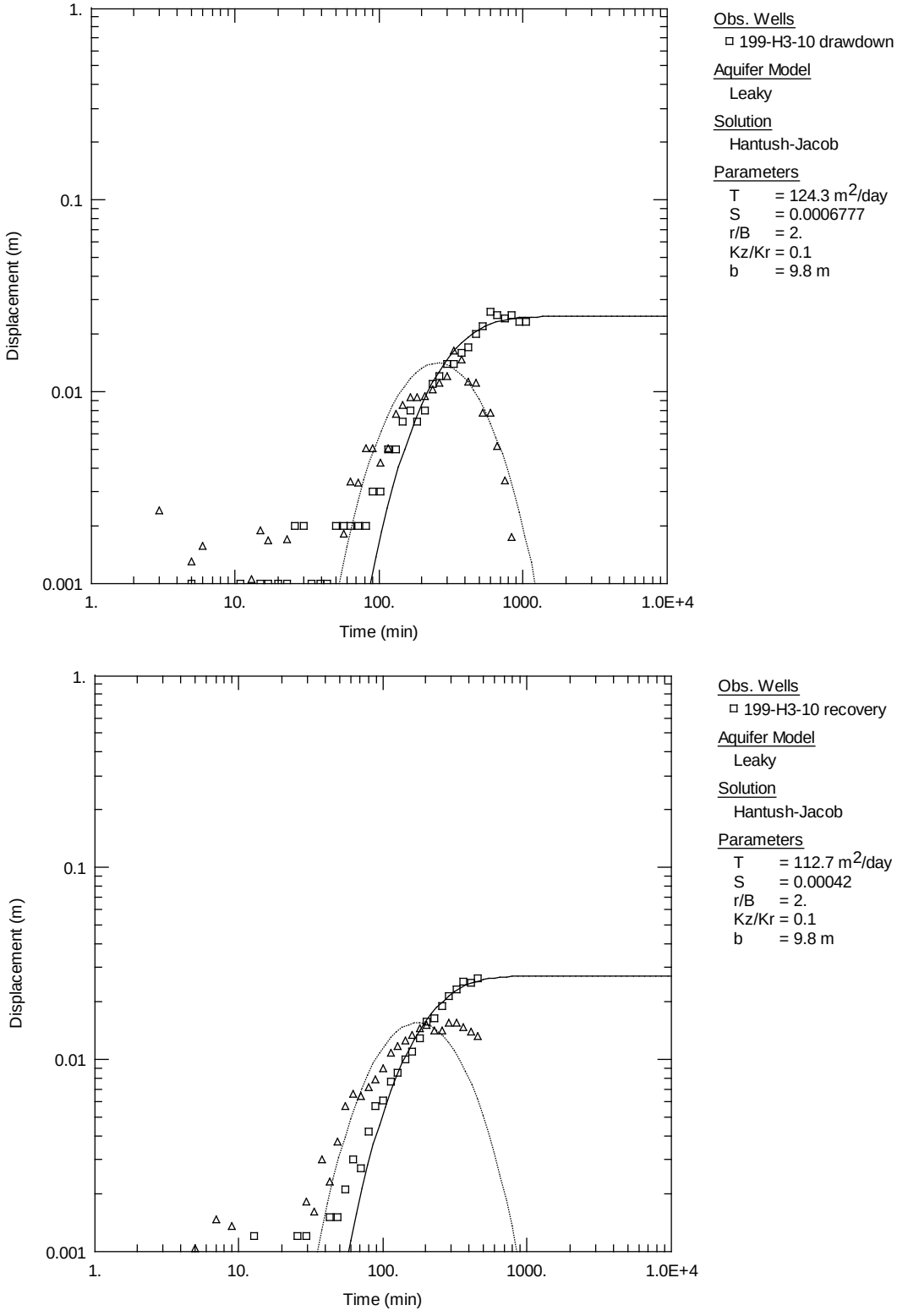

Figure A.10. Type-curve matches to the drawdown (upper plot) and recovery (lower plot) and derivative responses observed in well 199-H3-10 to the constant-rate pumping test in well 199-H3-22.

A.2 June 2019 P&T Shutdown Event Analysis Figures

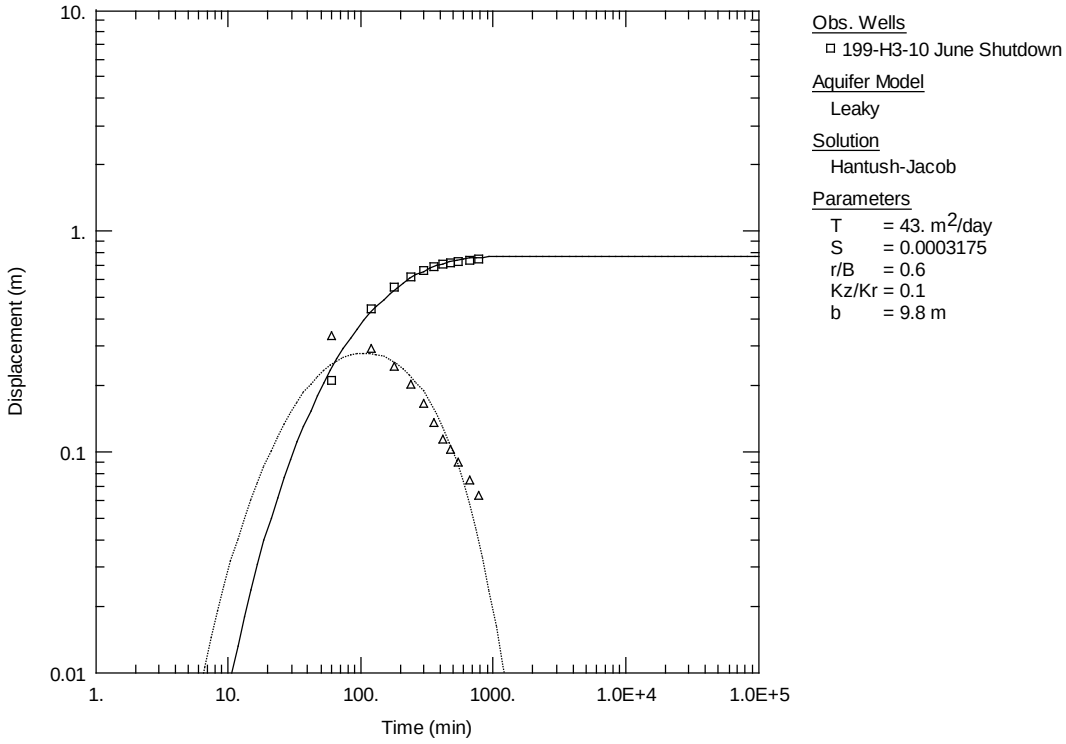

Figure A.11. Type-curve matches to the recovery and derivative responses observed in well 199-H3-10 to the June 2019 P&T shutdown event.

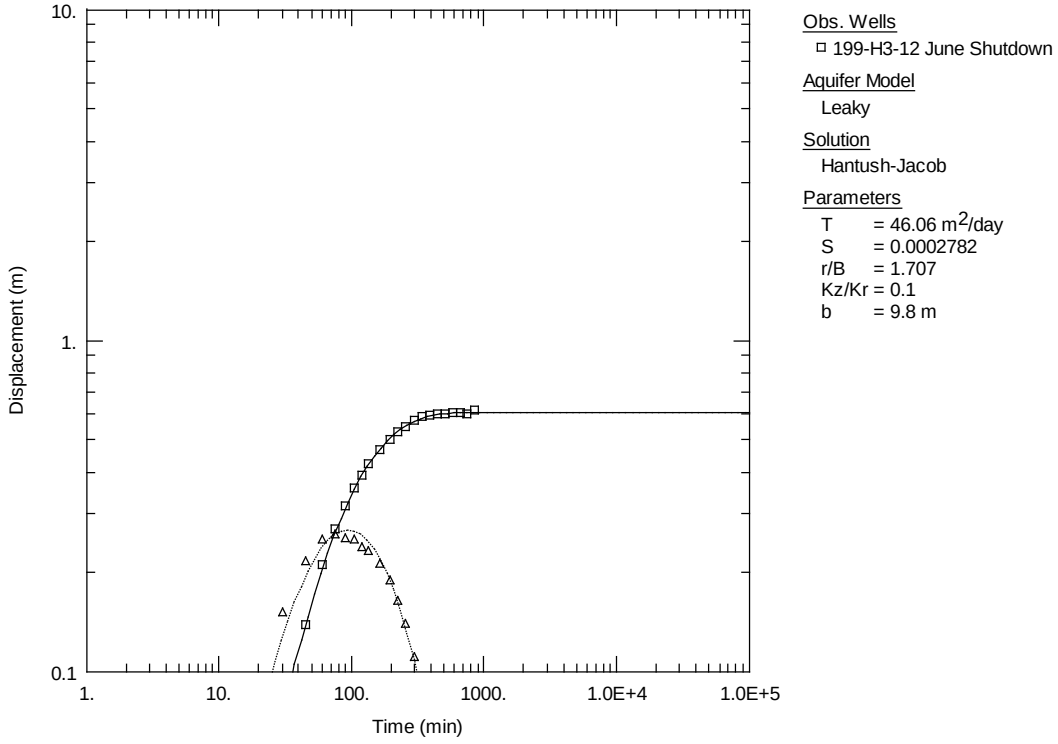

Figure A.12. Type-curve matches to the recovery and derivative responses observed in well 199-H3-12 to the June 2019 P&T shutdown event.

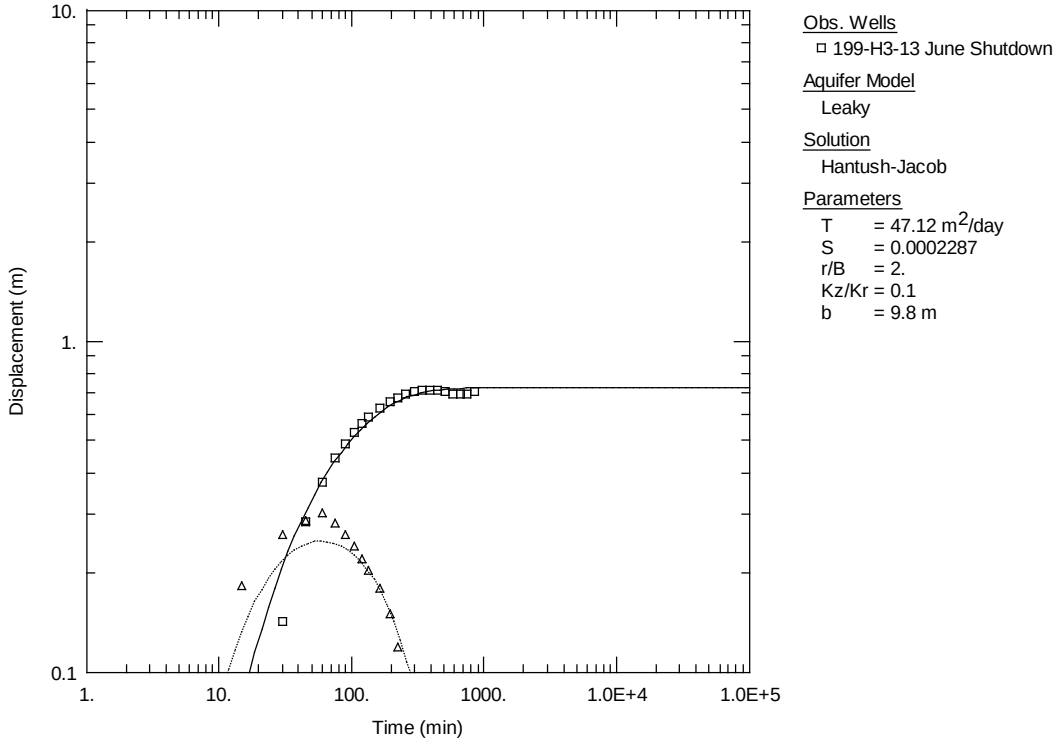

Figure A.13. Type-curve matches to the recovery and derivative responses observed in well 199-H3-13 to the June 2019 P&T shutdown event.

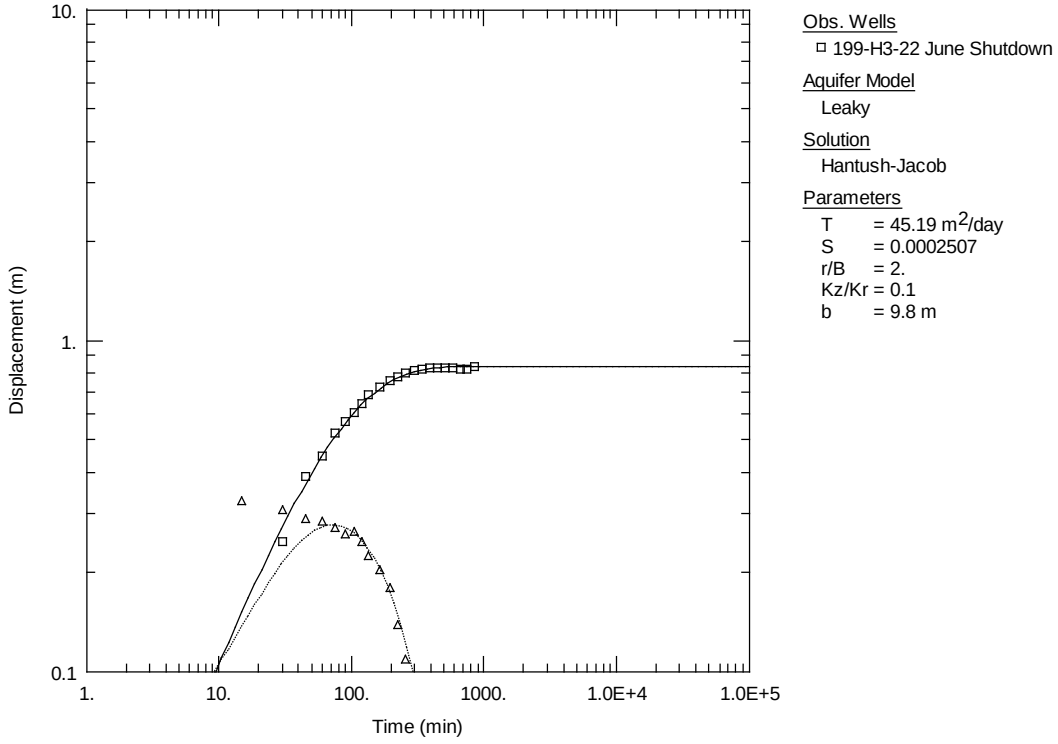

Figure A.14. Type-curve matches to the recovery and derivative responses observed in well 199-H3-22 to the June 2019 P&T shutdown event.

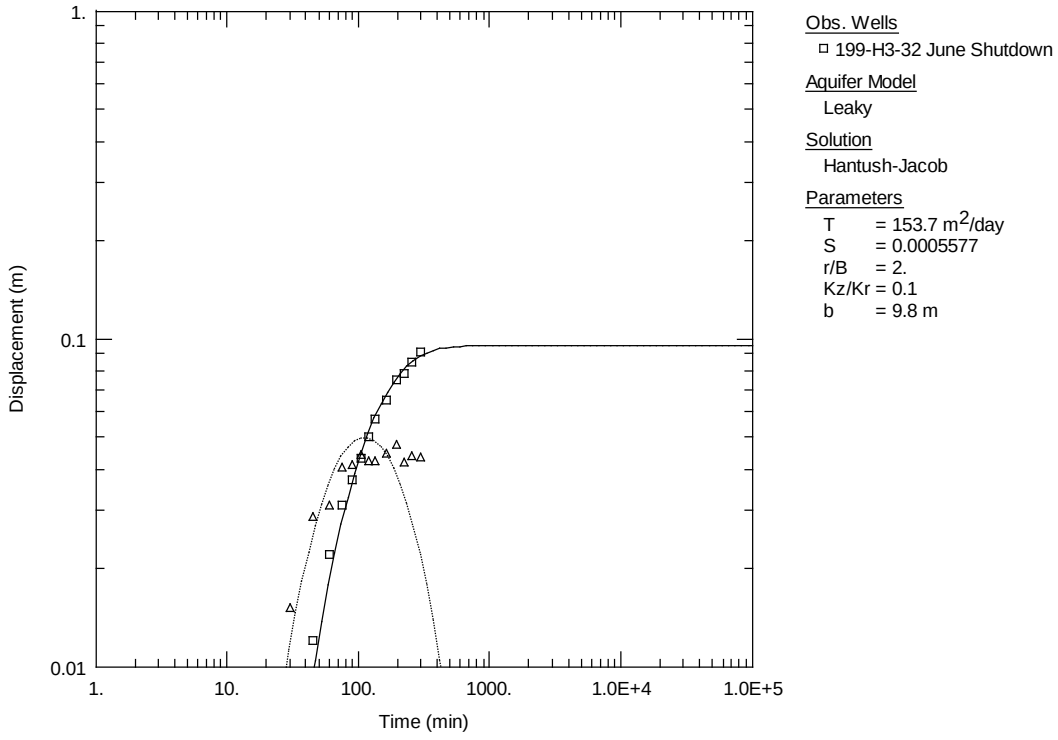

Figure A.15. Type-curve matches to the recovery and derivative responses observed in well 199-H3-32 to the June 2019 P&T shutdown event.

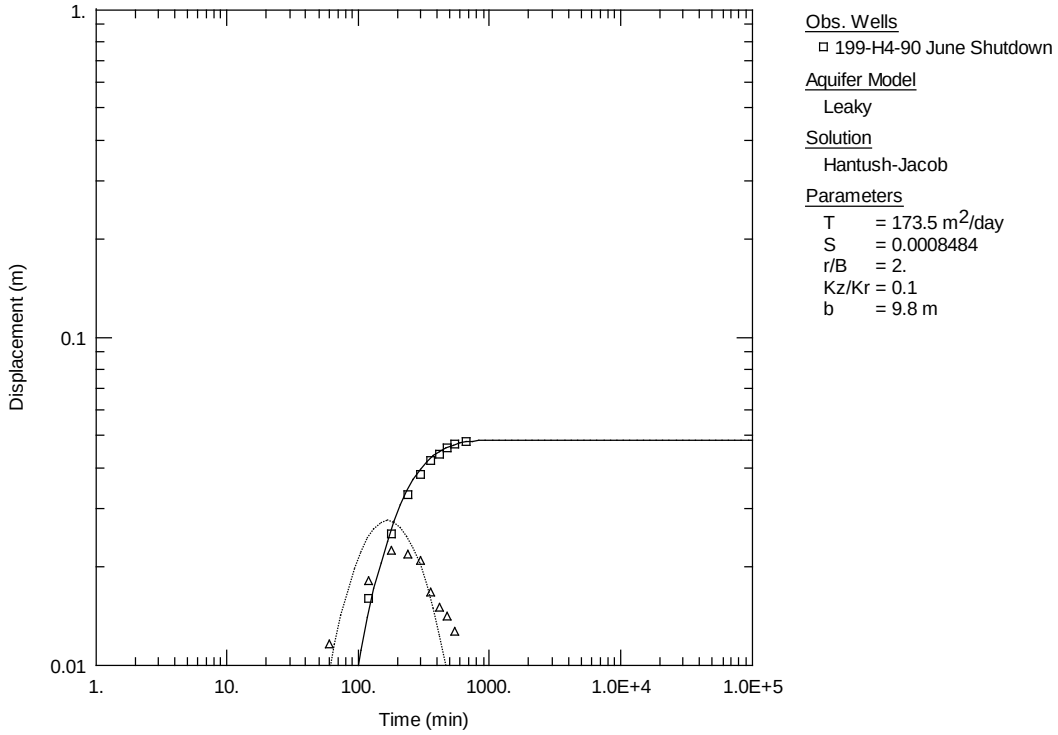

Figure A.16. Type-curve matches to the recovery and derivative responses observed in well 199-H4-90 to the June 2019 P&T shutdown event.

A.3 July 2019 P&T Shutdown Event Analysis Figures

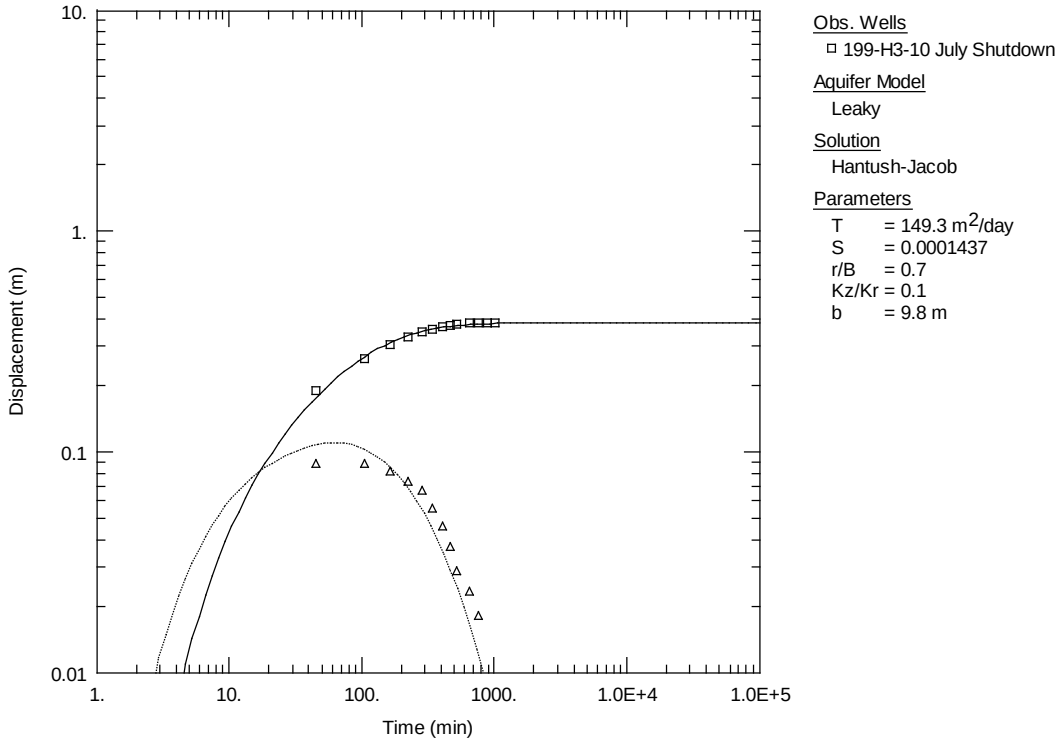

Figure A.17. Type-curve matches to the recovery and derivative responses observed in well 199-H3-10 to the July 2019 P&T shutdown event.

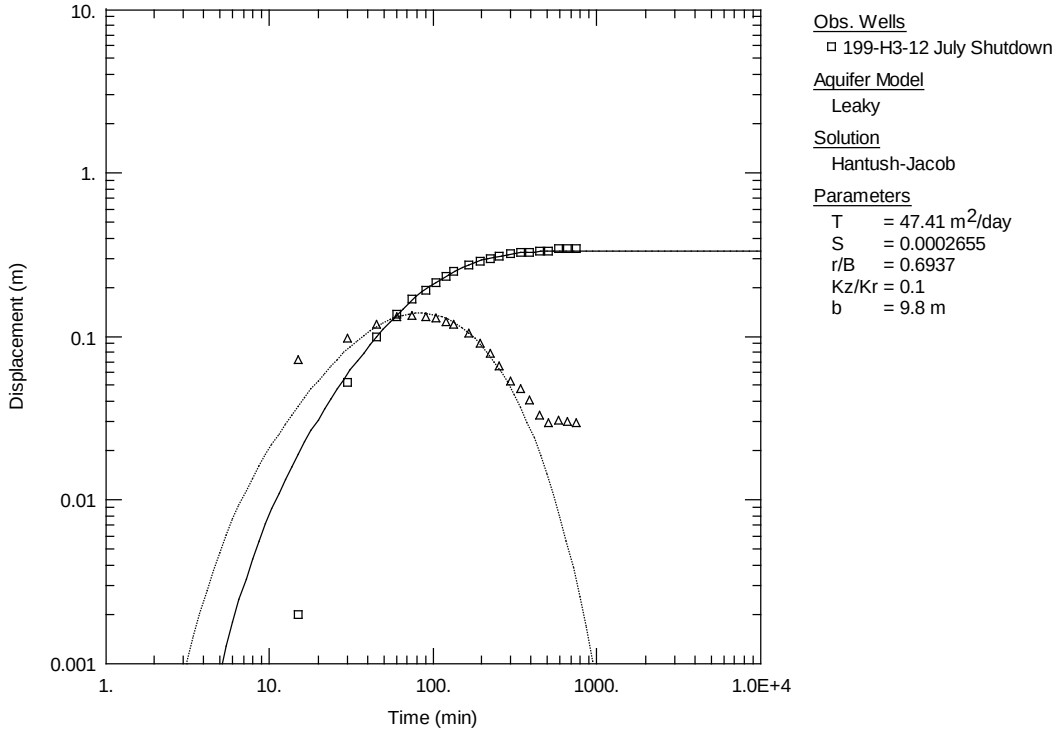

Figure A.18. Type-curve matches to the recovery and derivative responses observed in well 199-H3-12 to the July 2019 P&T shutdown event

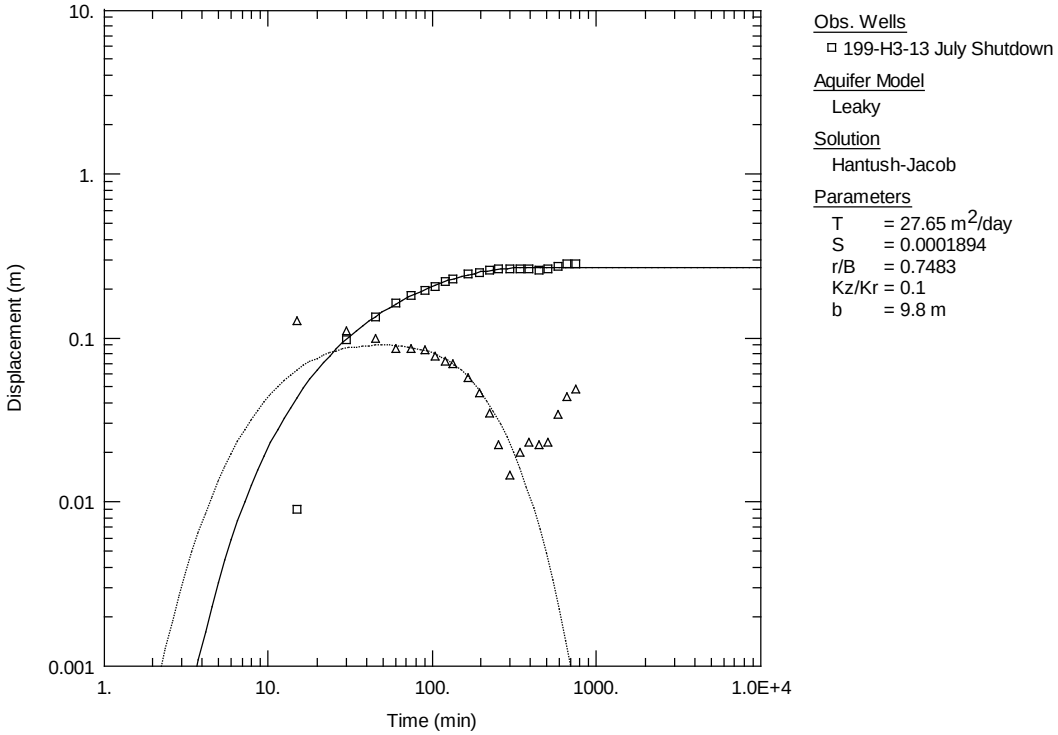

Figure A.19. Type-curve matches to the recovery and derivative responses observed in well 199-H3-13 to the July 2019 P&T shutdown event.

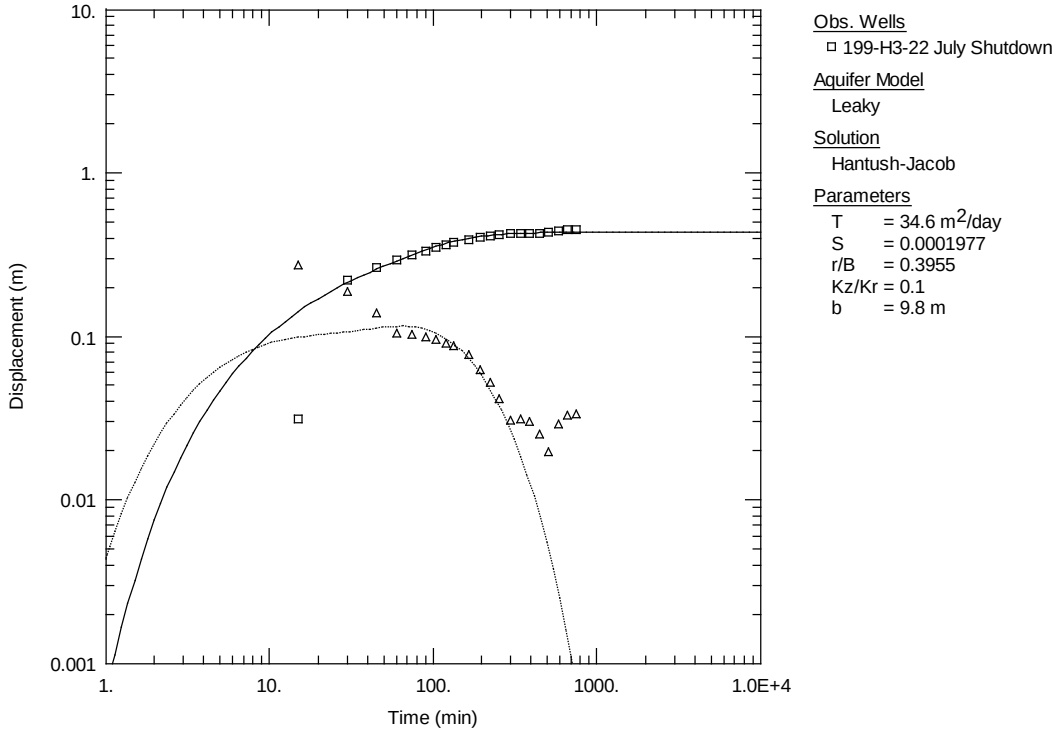

Figure A.20. Type-curve matches to the recovery and derivative responses observed in well 199-H3-22 to the July 2019 P&T shutdown event

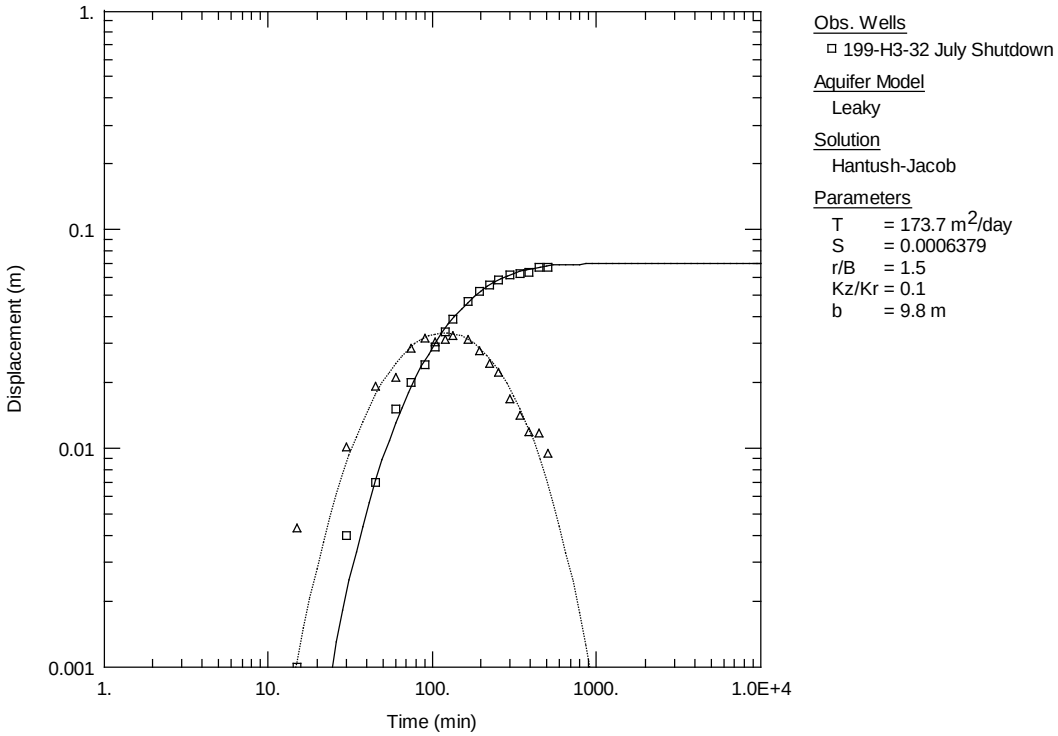

Figure A.21. Type-curve matches to the recovery and derivative responses observed in well 199-H3-32 to the July 2019 P&T shutdown event.

A.4 October 2019 P&T Shutdown Event Analysis Figures

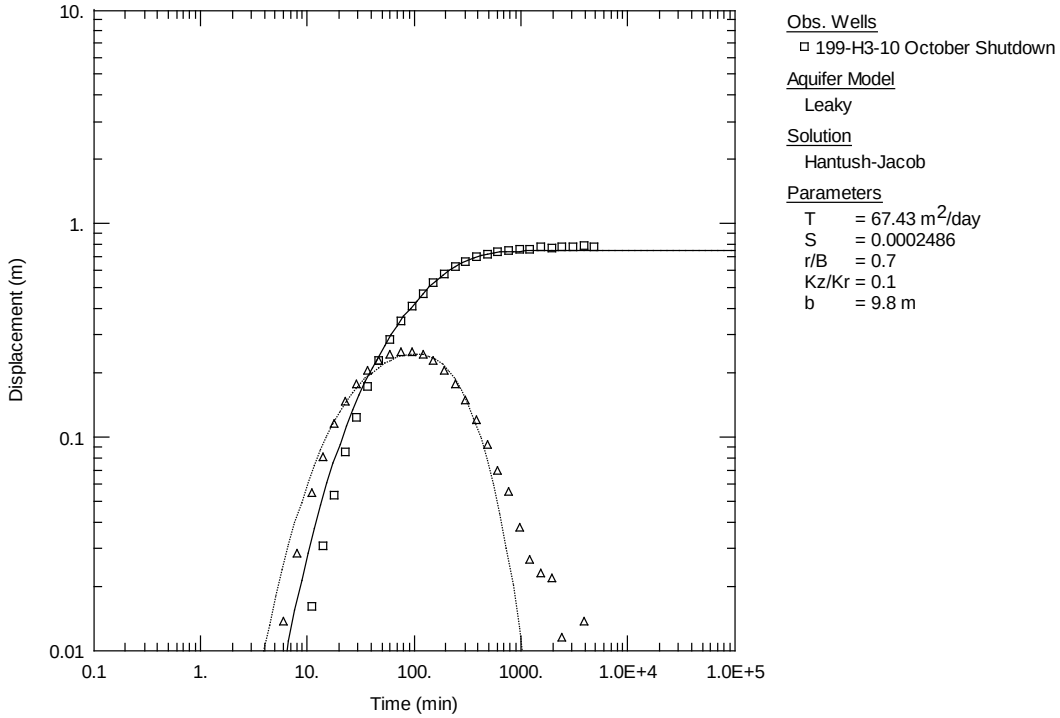

Figure A.22. Type-curve matches to the recovery and derivative responses observed in well 199-H3-10 to the October 2019 P&T shutdown event.

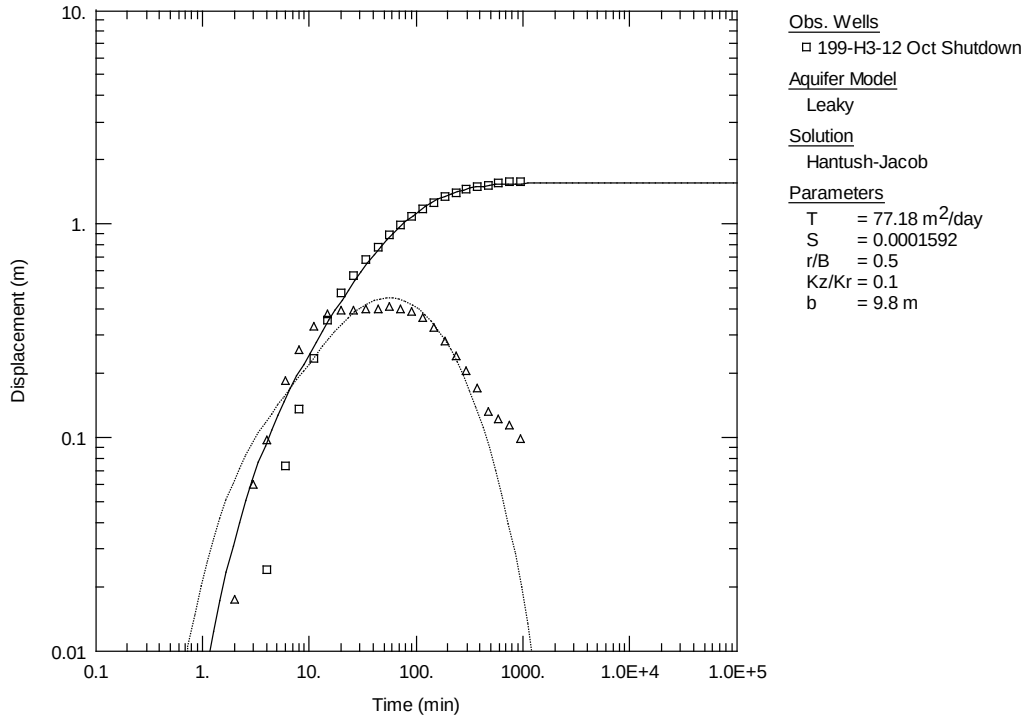

Figure A.23. Type-curve matches to the recovery and derivative responses observed in well 199-H3-12 to the October 2019 P&T shutdown event.

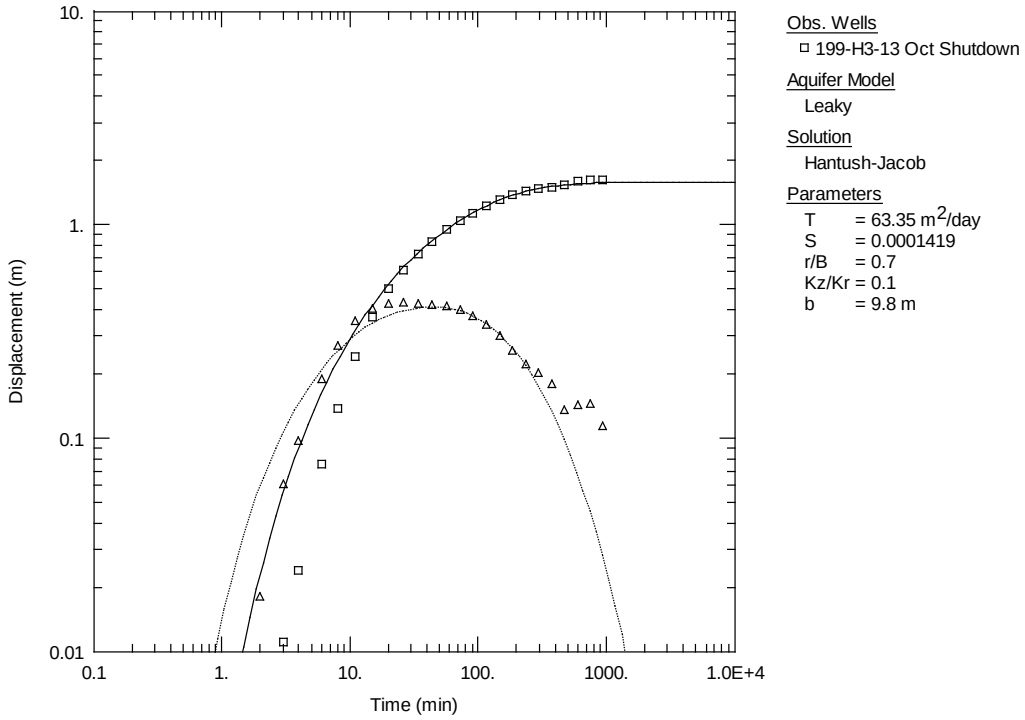

Figure A.24. Type-curve matches to the recovery and derivative responses observed in well 199-H3-13 to the October 2019 P&T shutdown event.

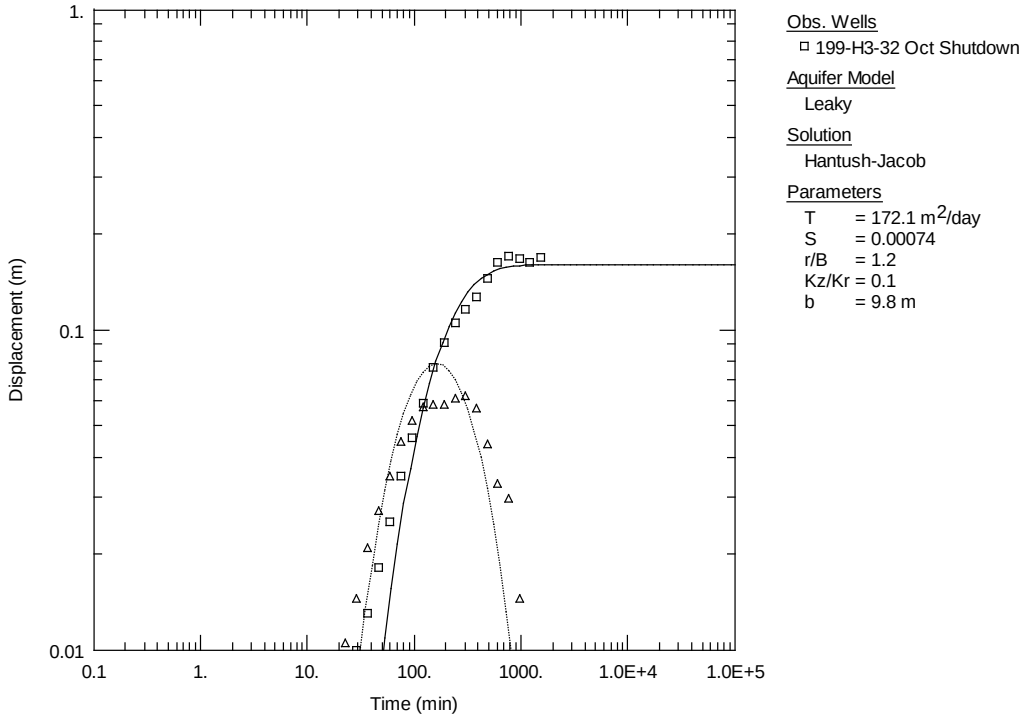

Figure A.25. Type-curve matches to the recovery and derivative responses observed in well 199-H3-32 to the October 2019 P&T shutdown event.

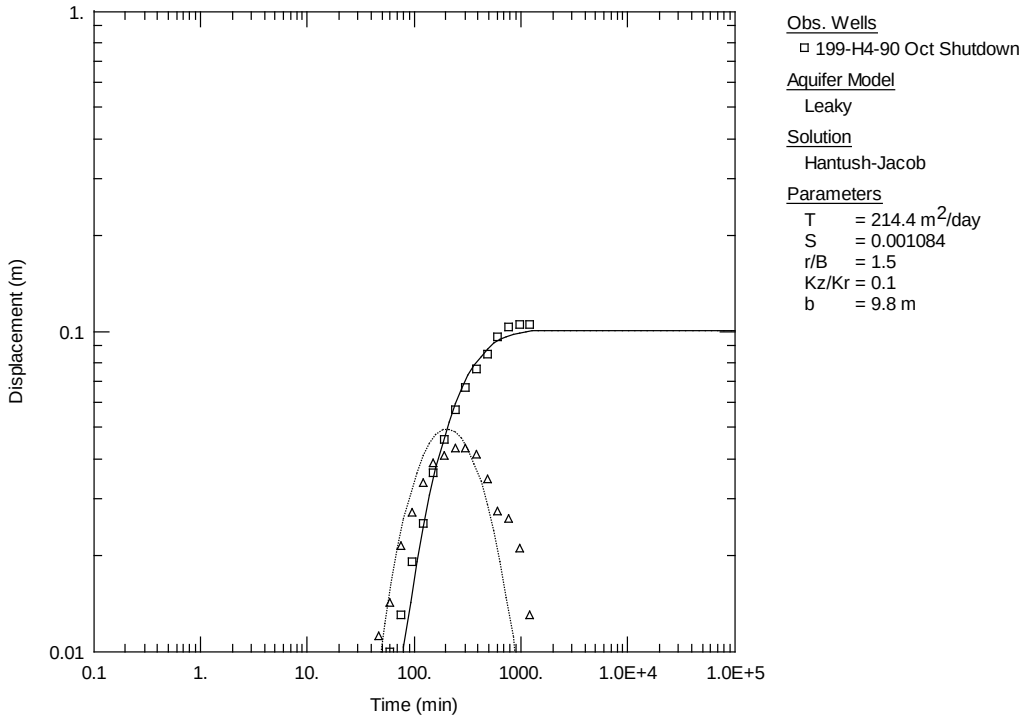

Figure A.26. Type-curve matches to the recovery and derivative responses observed in well 199-H4-90 to the October 2019 P&T shutdown event.

.

PNNL-30467

Pacific Northwest National Laboratory

902 Battelle Boulevard
P.O. Box 999
Richland, WA 99354
1-888-375-PNNL (7665)

www.pnnl.gov